Response to comments by referee 1

We would like to thank you for your comments and helpful suggestions. We revised our manuscript according to these comments and suggestions.

Specific comments:

This paper characterizes mixing layer height (MLH) over the major cities in the North China Plain based on the two-year surface observations. The relationship between MLH and regional air pollution is explored using concurrent PM, MLH, surface radiation, and meteorological parameters in the same cities. Overall, the paper is well written and the finding about the low MLH in southern Hebei is valuable to develop an efficient air pollution mitigation strategy in North China. I suggest the paper should be accepted by ACP after the authors address my comments below.

Comment 1:

It is not clear what is the difference between the MLH discussed here and the traditional defined planetary boundary layer height (PBLH). It would be interesting to see if the MLH obtained from surface can be inter-compared with PBLH from soundings like Guo J. et al. (2016).

Response 1:

Thank you for your helpful suggestion. Actually, we have already made comparisons between the MLH obtained from ceilometers and sounding data in Tang et al. (2016). The comparison results found that the ceilometers underestimate the MLH under conditions of neutral stratification caused by strong winds, whereas it overestimates MLH when sand-dust is crossing. When we excluded these two special weather conditions, the ceilometers observation results were fairly consistent with those retrieved from the sounding data. In addition, since the ceilometers can reflect the rainy conditions and precipitation will influence the MLH retrieval, data for precipitation were also excluded. In our study, data rectifications were made at the BJ, SJZ, TJ and QHD stations. The criterion to exclude these data points is as follows: (a) precipitation, i.e., a cloud base lower than 4000 m and the attenuated backscattering coefficient of at least 2×10^{-6} $m^{-1}sr^{-1}$ within 0 m and the cloud base, (b) sandstorm, i.e., the ratio of $PM_{2.5}$ to PM_{10} suddenly decreased to 30 % or lower and the PM_{10} concentration was higher than 500 μg m^{-3}, and (c) strong winds, i.e., a sudden change in temperature and wind speed when cold fronts passed by (Muñoz and Undurraga, 2010; Tang et al., 2016; Kamp and McKendry, 2010). Relevant contents were modified in section 2.2 in the revised manuscript.

Comment 2:

L266, the authors attribute the lower summertime MLH in QHD to the higher frequency of sea breeze. However, the underlying physical mechanism is not fully explained. Intuitively, the active sea breezes should come with more unstable atmosphere over the land. Figure 5 about prevailing wind directions in different seasons is referred, but it is still unclear to me how this figure supports the hypothesis above. Some detailed discussions are needed to better describe the formation and characteristics of the sea breeze in the coastal regions.

Response 2:

Thank you for your helpful suggestion. We are sorry for the unclear illustration about the impact of sea breezes. Here, we re-created the monthly diurnal wind vectors as shown below in Fig.1. We can see that the sea breeze usually started at midday (approximately 11:00 LT) and prevailed during daytime at the QHD station in spring and summer (Fig. 1d). The sea breeze usually brings a cold and stable air mass from the sea to the coastal region. Under the influence of the abrupt change of aerodynamic roughness and temperature between the land and sea surfaces, a thermal internal boundary layer (TIBL) will form in the coastal areas. Then, the local mixing layer will be replaced by the TIBL. Under the influence of warm air on land, the sea air advects downwind and warms, leading to a weak temperature difference between the air and the ground. In consequence, the TIBL warms less rapidly due to the decreased heat flux at the ground, and the rise rate is reduced. In addition, since the TIBL deepens with distance downwind and usually can not extend all the way to the top of the intruding marine air, the remaining cool marine air above the TIBL will hinder the TIBL vertical development (Stull, 1988; Sicard et al., 2006). As a result, the MLH at the QHD station was lower than other stations from April to September. Since the south-southwesterly wind impacts were enhanced in summer due to the weak synoptic systems, a frequent occurrence of the TIBL resulted in the lowest MLH at the QHD station in summer. To better illustrate the sea breeze impacts, we also made relevant modifications in section 4.1 in the revised manuscript.

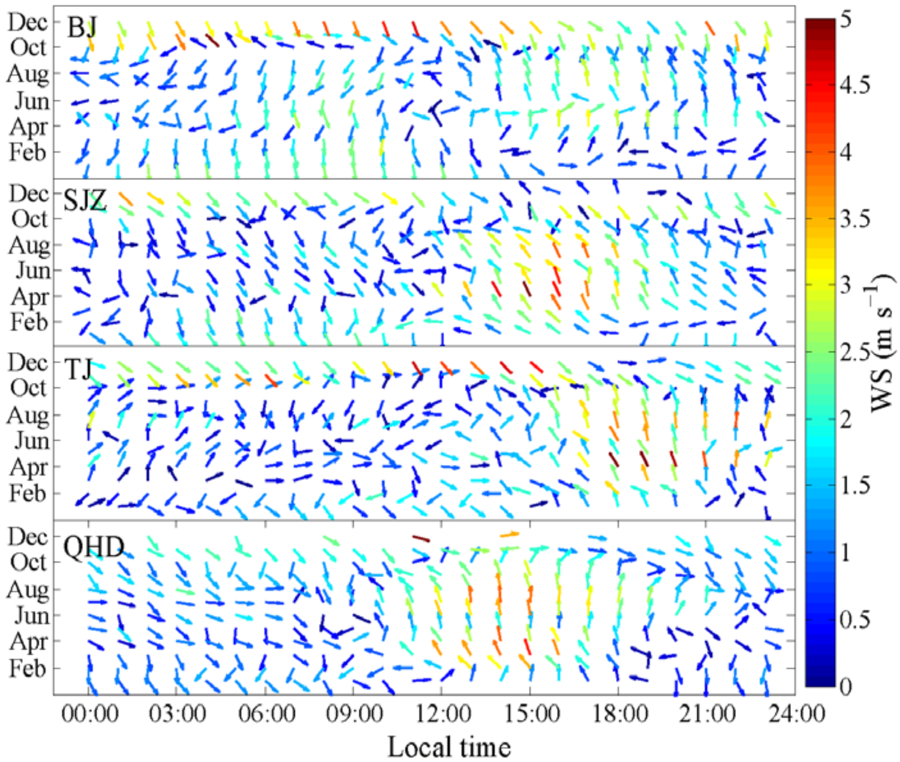

Fig. 1 Monthly variations of diurnal wind vectors at the BJ, SJZ, TJ and QHD stations from December 2013 to November 2014.

Comment 3:

L372, to overcome the lack of radio sounding in SJZ, how about directly using the reanalysis data? The quality of reanalysis can be evaluated by radio-sound at XT.

Response 3:

Thank you for your suggestion. We have made comparisons between reanalysis data and observation data at the Xingtai (XT) and Laoting (LT) stations, respectively. The reanalysis data were downloaded from the ECMWF website (http://apps.ecmwf.int/datasets/data/interim-full-mnth/levtype=pl/). As shown in Fig.2, there were large discrepancies between the two data sets. Meanwhile, the vertical resolution of the reanalysis data was too low to calculate the wind shear profile. Therefore, the reanalysis data could not be used to describe the meteorological parameter variations in this study. Considering the absence of vertical meteorological observations in other stations, comparisons of wind speed between the XT and Shijiazhuang (SJZ) stations, as well as LT and Qinhuangdao (QHD) stations were also made with the reanalysis data (Fig. 3). The wind speed between the XT and SJZ stations, and the LT and QHD stations were highly correlated, respectively, which indicated that the wind speeds in SJZ and QHD could be replaced by data in the XT and LT stations, respectively.

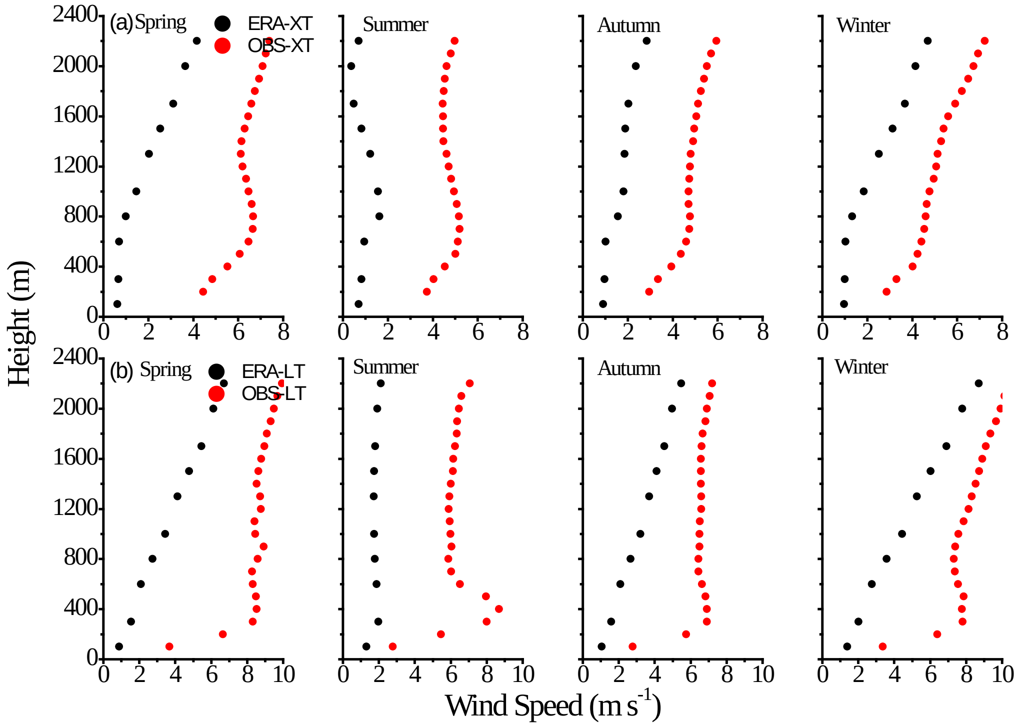

Fig. 2 Comparisons of seasonal wind speed profiles between the reanalysis and observation data at (a) the XT stations and (b) the LT stations.

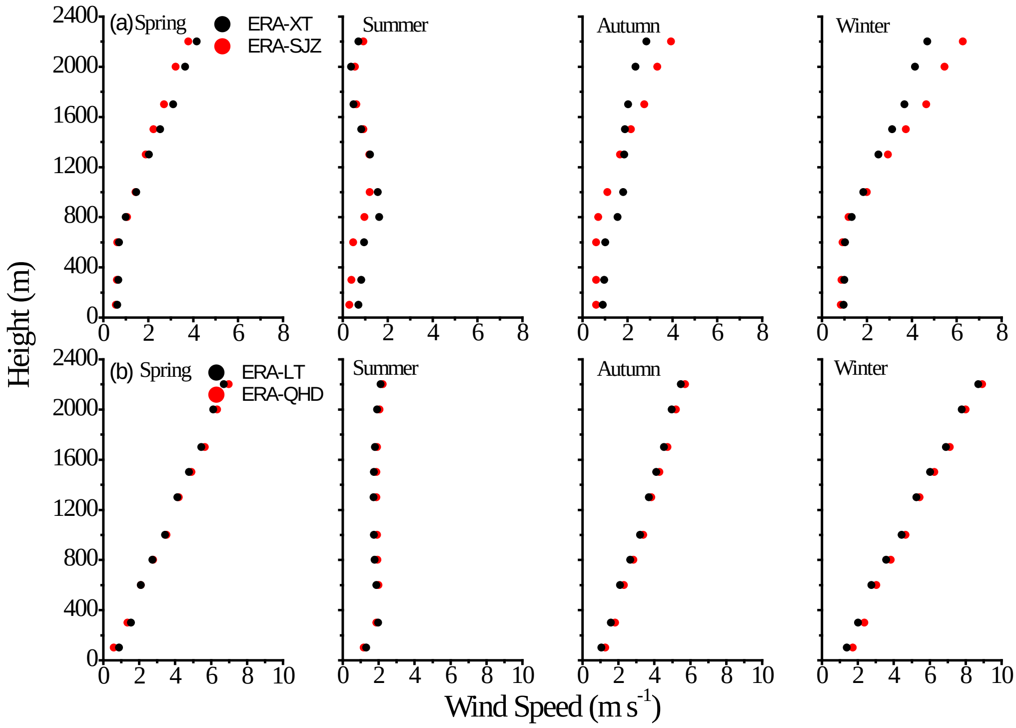

Fig. 3 Comparisons of seasonal wind speed profiles between the (a) XT and SJZ stations and the (b) LT and QHD stations with reanalysis data.

Comment 4:

Section 4.1, could absorbing aerosols be another factor to explain the reason of the low MLH in southern Hebei? Observations have revealed that the ambient aerosols can become highly absorptive in the urban conditions in China [Peng J. et al., 2016, PNAS]. The strong solar absorption near the top of PBL can increase the atmospheric stability and convective inhibition energy [Wang Y. et al., 2013, AE; Li Z. et al., 2016, Rev. Geos.]. Those possible influences from the feedback of air pollution should be discussed and quantified if possible.

Response 4:

Thank you for your constructive suggestion very much. We have read your mentioned papers and some other relevant research. Absorbing aerosols above the MLH can be another factor affecting the MLH because it gives rise to an increasing temperature aloft but a decreasing temperature at the surface, which will enhance the strength of capping inversion and inhibit the convective ability (Peng et al., 2016; Wang et al., 2013; Li et al., 2016). In contrast, absorbing aerosols within the mixing layer could reduce the capping inversion intensity despite the reduction in the surface buoyancy flux and raise the MLH (Yu et al., 2002). Considering the higher concentrations of surface $PM_{2.5}$ in southern Hebei, absorbing aerosols could likely have some impacts on MLH development. However, the comprehensive influences from the feedback of absorbing aerosols above and below the MLH are difficult to explain without sufficient knowledge of the vertical variations in absorbing aerosols. Although the near-ground absorbing aerosol concentration (such as black carbon) has regional differences (Zhao et al., 2013), the absorbing aerosol column concentrations could be consistent (Gong et al., 2017) with little difference in absorptive aerosol optical depths (AAOD). In addition, the mixed state and morphology of absorbing aerosols dominate the absorption effects (Jacobson, 2001; Bond et al., 2013). Therefore, without sufficient observation data, it is difficult to discuss and quantify the possible influences from the feedback of air pollution on the MLH development at present. Some elaborate experiments of vertical profiles and morphology need to be implemented in future studies. To compensate for this deficiency and inform readers of the uncertainties, the relevant contents were modified in section 4.2 in the revised manuscript.

Comment 5:

L437, what makes the RH at SJZ is higher than that in BJ and TJ? SJZ is more inland than those two cities.

Response 5:

Thank you for your suggestion. As shown in Fig. 4, seasonal distributions of near-ground RH from December 2013 to November 2014 in the NCP were depicted below. It was obvious that southern Hebei had higher RH than that in the northern NCP. The RH distribution was not only related to the distance from the sea but also to the flow fields and synoptic systems. This might result from the frequent passage of the Siberian High in the northern NCP, especially in spring and winter. In spring, when frequent sand storms occur, a dry air mass is brought to the northern NCP; thus the RH in the northern NCP was far less than that in southern Hebei (Fig. 4a). Meanwhile, under the impact of the Siberian High, a frequent weak northwest flow from Inner Mongolia will bring cold and dry air to the northern NCP in winter and autumn, and such north flow was too weak to reach southern Hebei (Su et al., 2004), which will lead to a lower RH in the northern NCP (Fig. 4c and 4d). In addition, the higher RH in southern Hebei could also be affected by the subtropical high (wet southeast flow) from the Yellow Sea.

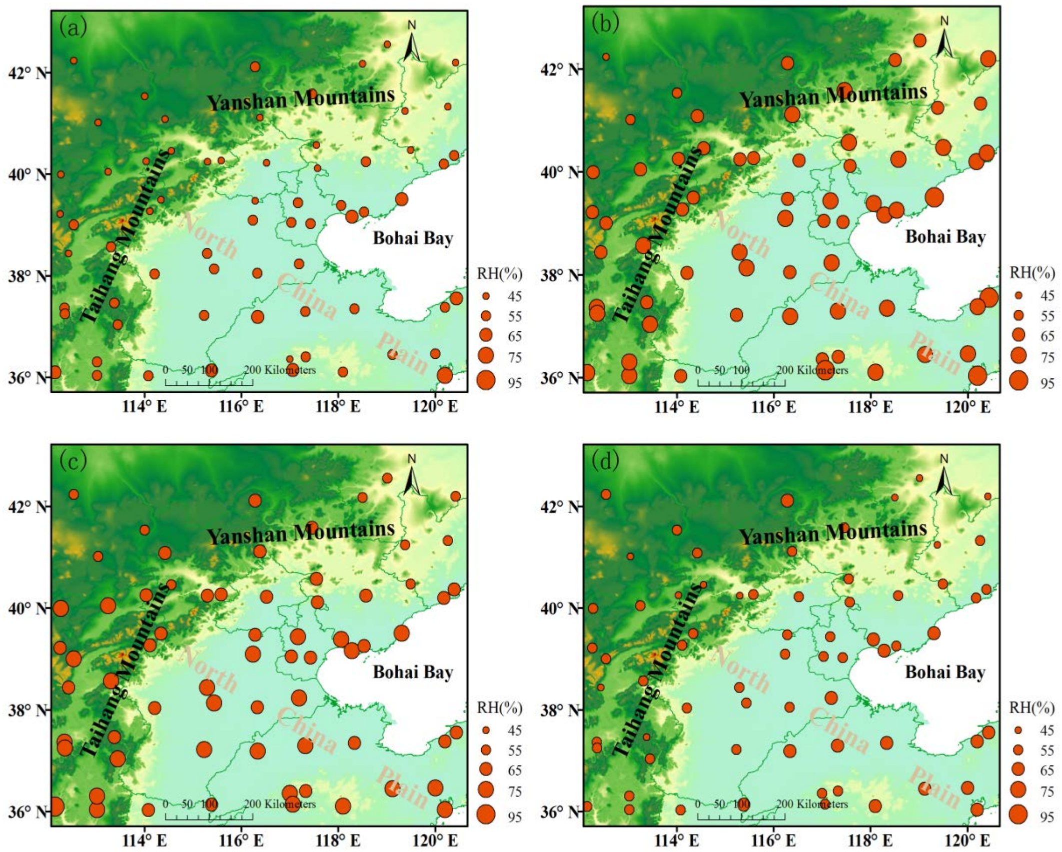

Fig. 4 Distributions of seasonal averaged RH in the NCP from December 2013 to November 2014: (a) spring, (b) summer, (c) autumn and (d) winter.

Comment 6:

L432-445, some basics of new particle formation in urban condition should be thoroughly reviewed. Please refer to Zhang, R. 2010, Science and 2015, Rev. Chem.

Response 6:

Thank you for your helpful suggestion. We apologize for our superficial understanding of the new particle formation and growth processes. We re-created some figures to illustrate the annual means of RH and T distributions over north China (Fig. 5). The T value in southern Hebei was similar to that in the northern NCP (Fig. 5a), which indicated an almost consistent temperature condition for an atmospheric chemical reaction between these two areas (Seinfeld J. and S. Pandis, 1998; Zhang et al., 2010; Zhang et al., 2015). However, differences existed in RH between southern Hebei and the northern NCP. The RH in southern Hebei was always higher than that in the northern NCP (Fig. 5b). As mentioned in our response to your comment 5, the Siberian and the subtropical high will be responsible for this RH distribution in the NCP region. Since the RH is a key factor for haze development, higher RH is beneficial to fine particle growth through the hygroscopic growth process and heterogeneous reaction. Relevant contents were modified in section 4.3.1 in the revised manuscript.

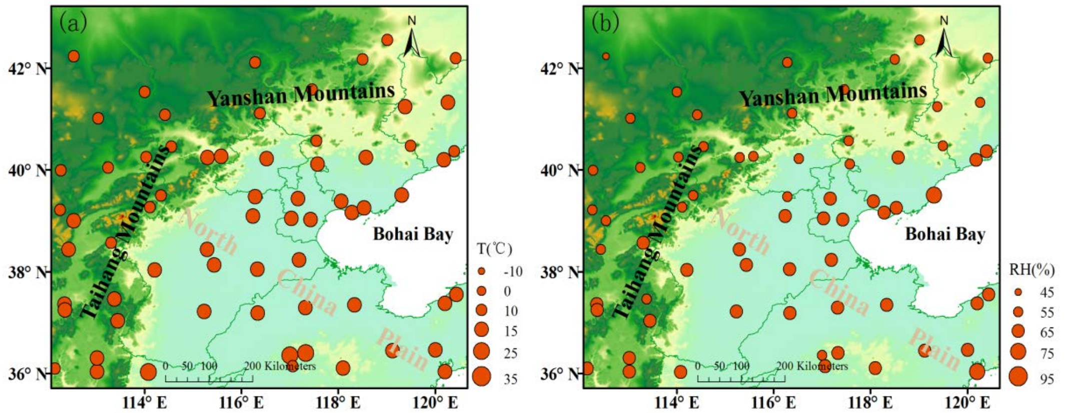

Fig. 5 Distributions of annual means of (a) T and (b) RH over the NCP region from December 2013 to November 2014.

Comment 7:

Fig. 8. Define V_c in the figure caption.

Response 7:

Thank you for your suggestion. We have already added the definition for V_c in the figure caption of Fig. 9 in the revised manuscript.

References:

Bond, T., S. Doherty, D. Fahery et al.: Bounding the role of black carbon in the climate system: a scientific assessment, J. Geophys. Res., 118, 1-173, doi:10.1002/jgrd.50171, 2013.

Gong, C., J. Xin, S. Wang, Y. Wang, T. Zhang: Anthropogenic aerosol optical and radiative properties in the typical urban/suburban regions in China, Atmos. Res., doi:10.1016/j.atmosres.2017.07.002, 2017.

Jacobson, M.: Strong radiative heating due to the mixing state of black carbon in atmospheric aerosols, Nature, 409,695-697, 2001.

Li, Z., W. Lau, and V. Ramanathan et al.: Aeosol and monsoon climate interactions over Asia, Rev. Geophys., 54, 886-929, doi:10.1002/2015RG000500, 2016.

Muñoz, R. and A. Undurraga: Daytime Mixing layer over the Santiago Basin: Description of Two Years of Observations with a Lidar Ceilometer, J. Appl. Meteorol. Clim., 49(8), 1728-1741, doi:10.1175/2010jamc2347.1, 2010.

Peng, J., M. Hu, S. Guo, Z. Du, J. Zheng, D. Shang, M. L. Zamora, L. Zeng, M. Shao, Y. Wu, J. Zheng, Y. Wang, C. R. Glen, D. R. Collins, M. J. Molina, and R. Zhang: Markedly enhanced absorption and direct radiative forcing of black carbon under polluted urban environments, P. Natl. Acad. Sci. Usa., 113(4266-4271), doi:10.1073/pnas.1602310113, 2016.

Seinfeld J. and S. Pandis: Atmospheric Chemistry and Physics: From Air Pollution to Climate Change, New York: John Wiley and Sons, 1998.

Sicard, M., C. Pérez, F. Rocadenbosch, J. Baldasano, and D. García-Vizcaino:

Mixed-Layer Depth Determination in the Barcelona Coastal Area From Regular Lidar Measurements: Methods, Results and Limitations. Boundary-Layer Meteorology 119, 135-157, 2006.

Stull, R.: An Introduction to Boundary Layer Meteorology, Kluwer Academic Publishers, Dordrecht, 1988.

Su, F., M. Yang, J. Zhong, Z. Zhang: The effects of synoptic type on regional atmospheric contamination in North Chian, Res. Of Environ. Sci., 17(3), doi:10.13198/j.res.2004.03.18.sufq.006, 2004.

Tang, G., J. Zhang, X. Zhu, T. Song, C. Münkel, B. Hu, K. Schäfer, Z. Liu, J. Zhang, L. Wang, J. Xin, P. Suppan, and Y. Wang, Mixing layer height and its implications for air pollution over Beijing, China, Atmospheric Chemistry and Physics, 16, 2459-2475, doi:10.5194/acp-16-2459-2016, 2016.

Kamp, V., and I. McKendry: Diurnal and Seasonal Trends in Convective Mixed-Layer Heights Estimated from Two Years of Continuous Ceilometer Observations in Vancouver, BC, Bound.-Lay. Meteorol., 137(3), 459-475, doi:10.1007/s10546-010-9535-7, 2010.

Wang, Y., M. Zamora, and R. Zhang: New Directions: Light absorbing aersols and their atmospheric impacts, Atmos. Environ., 81, 713-715, doi: 10.1016/j.atmosenv.2013.09.034, 2013.

Wei, J., G. Tang, X. Zhu, L. Wang, Z. Liu, M. Cheng, C. Münkel, X. Li and Y. Wang: Thermal internal boundary layer and its effects on air pollutants during summer in a coastal city in North China, Journal of Environmental Sciences, 1001-0742, doi:10.1016/j.jes.2017.11.006, 2017.

Yu, H., S. Liu, and R. Dickinson: Radiative effects of aerosols on the evolution of the atmospheric boundary layer, J. Geo. Res.: Atmos., 107, D12(4142), doi:10.1029/2001JD000754, 2002.

Zhang, R., G. Hui, S. Guo, M. Zamora, Q. Ying, Y. Lin, W. Wang, M. Hu, and Y. Wang: Formation of Urban Fine Particulate Matter, Chem. Rev., 115, 3803-3855, doi: 10.1021/acs.chemrev.5b00067, 2015.

Zhang, R.: Getting to the Critical Nucleus of Aerosol Formation, Science, 328(5984), 1366-1367, doi: 10.1126/science.1189732, 2010.

Zhao, P., F. Dong, Y. Yang, D. He, X. Zhao, W. Zhang, Q. Yao, and H. Liu: Characteristics of carbonaceous aerosol in the region of Beijing, Tianjin, and Hebei, China, Atmos. Environ., 71, 389-398, doi: 10.1016/j.atmosenv.2013.02.010, 2013.

Response to comments by referee 2

We would like to thank you for your comments and helpful suggestions. We revised our manuscript according to these comments and suggestions.

Specific comments:

This study reveals the spatial variation of mixing layer height (MLH) over northern China plain (NCP) based on a two-year measurement at four primary cities with different geographic allocation across NCP. The authors attribute the different spatial pattern of MLH between southern Hebei and northern NCP to the distinct wind shear features between the two interested regions. The analysis on the long-term measurement of MLH in this study provides a meaningfully insight on the climatological features of boundary layer condition during the haze episodes over NCP. Also, the discussions about the associations of MLH and other meteorological factors with the near-ground particle pollution are sufficiently presented in this work. However, the following concerns should be addressed before publication.

Comment 1:

Considering the possible strong aerosol-radiation interaction because of the heavily pollution, the surface net radiation is supposed to be lower over the regions with more heavily pollution because of the strong scattering and/or absorbing of solar radiation by aerosols. However, in this study, though the near-ground $PM_{2.5}$ concentration over southern Hebei is 1.3 times higher than that of north China plain (NCP), there is no significant difference in the net radiation at Shijiazhuang (SJZ) located southern Hebei from at Beijing (BJ) located over NCP. One probable reason is because the aerosol optical depth (AOD) over the two sites was comparable, leading to comparable capacity reducing solar radiation. The authors may check the AOD data to obtain a convinced explanation for why the net radiation is spatial consistent, given the presence of aerosol-radiation interaction.

Response 1:

Thank you for your helpful suggestion. We have checked the AOD distribution in the NCP as you suggested. The AOD data were retrieved with the dark target algorithm from the Moderate Resolution Imaging Spectra-radiometer (MODIS) aerosol products on board the NASA EOS (Earth observing system) Terra satellite. As shown in Fig. 1 below, the AOD in Shijiazhuang (SJZ) was 1.1 and 1.0 times higher than that at the Beijing (BJ) and Tianjin (TJ) stations, respectively. Given the presence of aerosol-radiation interaction, the comparative amount of AOD could be one probable reason to explain the nearly consistent net radiation between the SJZ and BJ stations. In our revised manuscript, the net radiation analysis was replaced by gradient Richardson number (*Ri*) studies, and *Ri* is a better index that can evaluate the atmospheric stability from both the perspectives of thermal and mechanism forces. Then, the low mixing layer height (MLH) in winter in southern Hebei mainly resulted from the stable turbulent stratification (using summer and winter as examples) (Fig.1). Relevant contents were modified in section 4.2 in the revised manuscript. In addition, we discovered some new findings when the AOD analysis was added in the discussion. Please refer to comment 2.

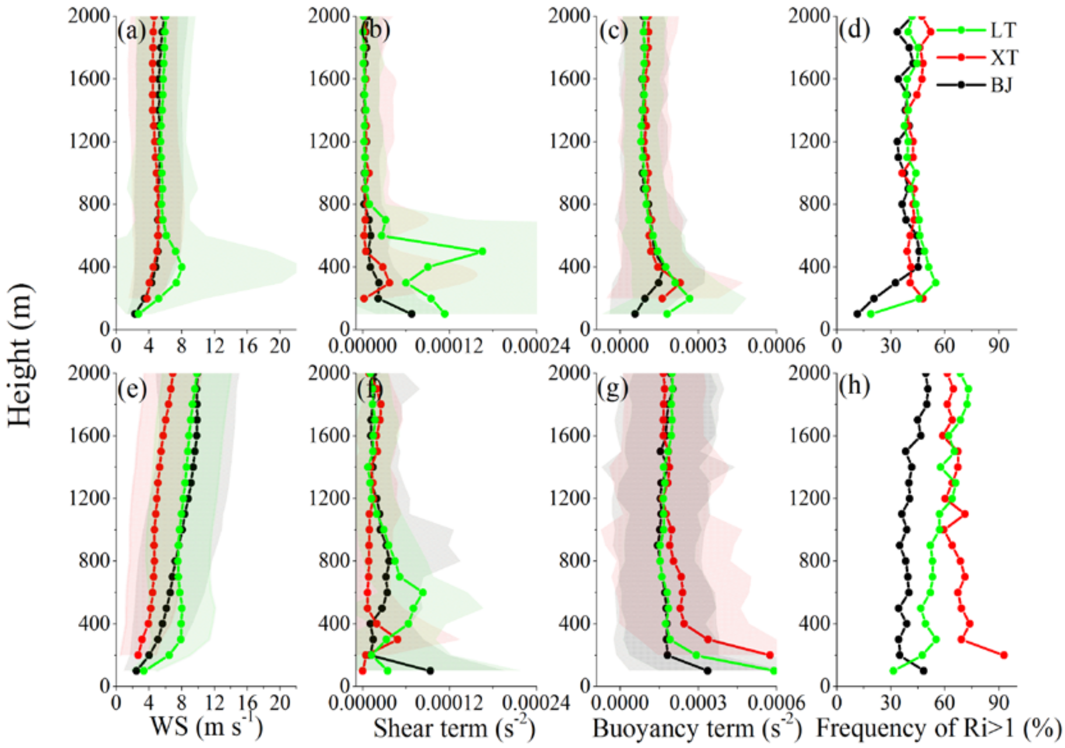

Fig.1 Vertical profiles of (a, e) the horizontal WS, (b, f) the shear term, (c, g) the buoyancy term and (d, h) the percentage of *Ri*>1 at the BJ, XT and LT stations in summer (upper panel) and winter (lower panel).

Comment 2:

In addition to the difference in mixing layer height (MLH), how likely does the spatial variation in pollutant emissions contribute to the difference in the near-ground PM pollution between SJZ and BJ?

Response 2:

Thank you for your suggestion. Since the particle has direct emission sources and secondary sources, and the distribution of direct emissions cannot represent the total contribution of emissions to the particle concentration. The near-ground $PM_{2.5}$ concentration could represent the particle concentrations at the ground, but considering that the particle lifetime is much longer than that of trace gases, the particle concentrations are nearly uniform in the mixing layer because of the strong vertical mixing. Therefore, near-ground $PM_{2.5}$ concentrations cannot be used to evaluate the emissions influences between different regions if the mixing layer heights are different. AOD, which represents the aerosol column concentration, is a much better indicator for the emissions difference. As shown in Fig. 2, the major sites in southern Hebei (the SJZ, Handan (HD) and Xingtai (XT) stations) and the northern NCP (the BJ and TJ stations) were enclosed with white rectangles. The average AOD value at the southern Hebei stations was 1.2 times higher than the AOD at the northern NCP regions, while the near-ground $PM_{2.5}$ concentration in southern Hebei was 1.5 times higher than that in the northern NCP. If the AOD difference represents the emission discrepancy, the remaining differences of $PM_{2.5}$ concentration may be induced by the meteorology. In other words, except for the emission effect, the meteorological conditions also play an important role in pollutant contrast between these two areas. Relevant contents were also modified in section 4.3 in our revised manuscript.

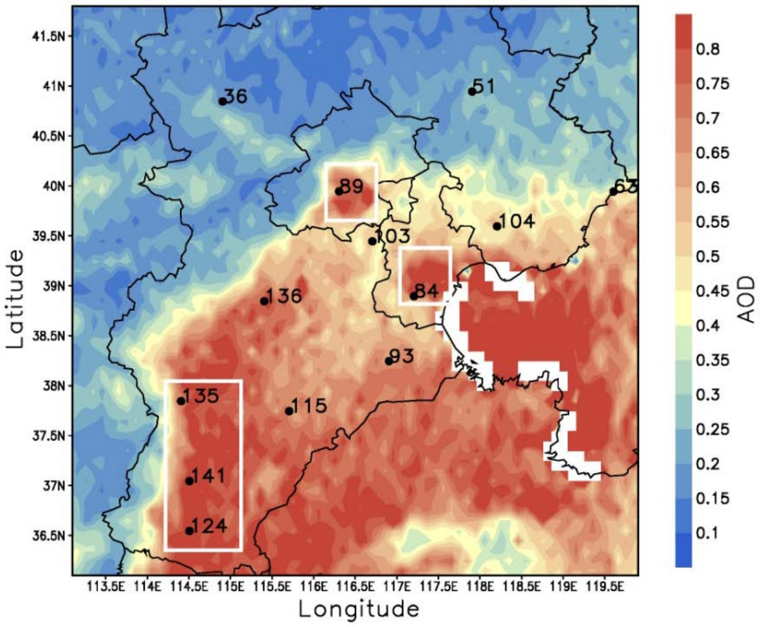

Fig. 2 AOD distribution from December 2013 to November 2014 in the NCP. The $PM_{2.5}$ concentrations of the 13 observation sites were also marked beside each station. Major sites in the northern NCP (BJ and TJ) and southern Hebei (SJZ, XT and HD) were enclosed by white rectangles.

Comment 3:

The authors attribute the spatial difference in wind shear over NCP during winter to the influence of front passing associated with the Siberian High (lines 403-405). Is the front also the dominant control of the relative humidity over NCP during winter? Is there any other reason leading to the discrepancy in relative humidity between the two regions in question?

Response 3:

The spatial difference in wind shear over the NCP in spring, autumn and winter probably resulted from the more frequent weak cold air impact on the northern NCP region. When the cold air was brought by a high-pressure system, the cold front formed and enhanced the wind shear in BJ. However, in summer, due to the northward lift and westward intrusion of the subtropical high on the NCP, the diminished effect of the weak cold air on the northern NCP accompanied with strong solar radiation and turbulent activities will lead to less wind shear contrast in the vertical direction between southern Hebei and the northern NCP. Certainly, the front is also the dominant control of the RH over the NCP. In addition, higher RH in southern Hebei might result from the frequent passage of the Siberian High in the north NCP, especially in spring and winter. In spring, when frequent sand storms occur, a dry air mass is brought to the northern NCP; thus, the RH in the northern NCP was far less than that in southern Hebei (Fig. 3a). Meanwhile, under the impact of the Siberian High, a frequent weak northwest flow from Inner Mongolia will bring cold and dry air to the northern NCP in winter and autumn, and such north flow was usually too weak to reach southern Hebei (Su et al., 2004), which will lead to lower RH in the northern NCP (Figs. 3c and 3d). In addition, the higher RH in southern Hebei could also be affected by the subtropical high (wet southeast flow from the Yellow Sea).

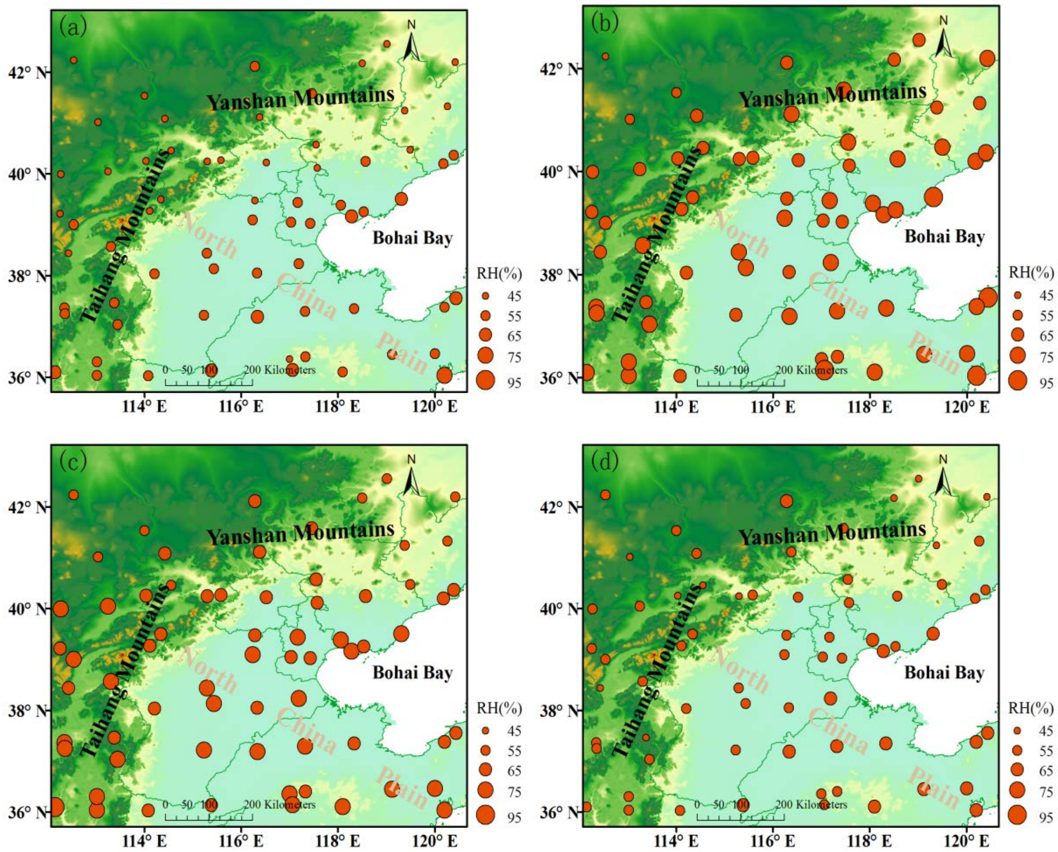

Fig. 3 Distributions of seasonal averaged RH in the NCP from December 2013 to November 2014: (a) spring, (b) summer, (c) autumn and (d) winter.

Comment 4:

Given that both Tianjin (TJ) and Qinhuangdao (QHD) are located at coastal region and suffering highly frequent sea breezes during summer (Fig. 5), why the MLH of TJ is much higher than the case in QHD, since the relatively low MLH in QHD is attributed by the authors to the intensive occurrence of sea breeze during summer (lines 265-266)?

Response 4:

Thank you for your suggestion, and we apologize for our unclear description. Actually, the MLH at the coastal region was affected by the thermal internal boundary layer (TIBL), not the sea breeze. When the cold air mass came with the sea breeze and the top of the mixing layer was higher than the top of the air mass, the TIBL will form within the original mixing layer, interrupting the original mixing layer development and decreasing the MLH. With distance inland, the top of the sea air mass will enhance and exceed the local MLH; if so, the TIBL will not form, and the TIBL impact will be impaired with distance inland (Stull, 1988). Since the QHD station was only 2 km away from the coastline and the distance of the TJ station was approximately 50 km out to sea, the TIBL will not form in the TJ station. The MLH variation for TJ was the same with those inland sites (BJ and SJZ). The relevant contents were modified in section 4.1 in our revised manuscript.

Technical comments:

Comment 1:

Fig. 7: the unit for the wind shear should be m s-1 km-1.

Response 1:

Since the $\text{wind shear} = \sqrt{\left(\frac{\Delta \bar{u}}{\Delta z}\right)^2 + \left(\frac{\Delta \bar{v}}{\Delta z}\right)^2}$ and the unit of wind speed and Δz was m s^{-1} and m, respectively, the unit of wind shear was m $s^{-1}m^{-1}$. The study of wind shear was replaced by the study of shear term $(\left(\frac{\Delta \bar{u}}{\Delta z}\right)^2 + \left(\frac{\Delta \bar{v}}{\Delta z}\right)^2)$ in our revised manuscript. And to be consistent with the unit of buoyancy term, the unit of shear term was s^{-2}.

Comment 2:

The descriptions on Figs. 5c and 5d in lines 320-322 seems not consistent with what was shown in figure. For example, the prevailed wind direction during spring and summer for TJ is southerly as shown in Fig. 5c, which is not the case stated by the text in lines 320-322, i.e. easterly wind is prevailed in TJ.

Response 2:

Thank you for your suggestion, and we have already modified the relevant descriptions in section 4.1 in the revised manuscript.

References:

Stull, R.: An Introduction to Boundary Layer Meteorology, Kluwer Academic Publishers, Dordrecht, 1988.

Su, F., M. Yang, J. Zhong and Z. Zhang: The effects of synoptic type on regional atmospheric contamination in North Chian, Res. Of Environ. Sci., 17(3), doi:10.13198/j.res.2004.03.18.sufq.006, 2004.

Response to short comments

We would like to thank you for your comments and helpful suggestions. We revised our manuscript according to these comments and suggestions.

Specific comments:
The climatology of MLH at four sites over NCP was investigated using long-term measurements. However, lots of statements in the manuscript and part of conclusions were not well supported. Thus, a major revision is suggested.

Comment 1:
LINE 214-215, the definitions of rainy, sandstorm and windy conditions should be given.

Response 1:
Thank you for your suggestion. The criteria to exclude the data points for special conditions are as follows: (a) precipitation, i.e., a cloud base lower than 4000 m and an attenuated backscattering coefficient of at least 2×10^{-6} $m^{-1}sr^{-1}$ within 0 m and the cloud base, (b) sandstorm, i.e., the ratio of $PM_{2.5}$ to PM_{10} suddenly decreased to 30 % or lower and the PM_{10} concentration was higher than 500 μg m^{-3}, and (c) strong winds, i.e., a sudden change in temperature and wind speed when cold fronts passed by. We also modified the relevant contents in section 2.2 in the revised manuscript.

Comment 2:
LINE 317-318, “the TJ station was supposed to be an inland site”, the TJ site is quite close to the Bohai sea, which should be considered as a coastal station.

Response 2:
Actually, the Tianjin (TJ) site was set in the courtyard of the Tianjin Meteorological Bureau, which was located south of the urban area (117.20°E, 39.13°N) with approximately 50 km away from the coast. The Qinhuangdao (QHD) station was set up in the Environmental Management College of China (119.57°E, 39.95°N) with only approximately 2 km away from the coastline. Therefore, the TJ site, by contrast, was supposed to be an inland site. In addition, the mixing layer height (MLH) at the coastal region was affected by the thermal internal boundary layer (TIBL), not the sea breeze. When the cold air mass came with the sea breeze and the top of the mixing layer was higher than the top of the air mass, the TIBL will form within the origin mixing layer, interrupt the origin mixing layer development and decrease the MLH. With distance inland, the top of the sea air mass will enhance and exceed the local MLH; if so, the TIBL will not form, and the TIBL impact will be impaired with distance inland (Stull, 1988). Since the QHD station was only 2 km away from the coastline and the distance of the TJ station was approximately 50 km out to sea, the TIBL will not form in the TJ station. The MLH variation for TJ was the same with those inland sites. The relevant contents were modified in section 4.1 in our revised manuscript. From another point of view, the definition of a coastal station should be the one that was affected by the TIBL.

Comment 3:
LINE 319-324, the definition of sea-breeze used in this study should be given. The sea-breeze cannot be identified merely by the near-surface wind speed and direction. How to identify the sea-breeze from background wind? How to calculate the occurrence frequency of sea-breeze at TJ and QHD?
Response 3:
Thank you for your suggestion. The sea-land breeze was a local circulation; it occurs when there is no large scale synoptic system that passes. In our study, we first exclude days with large-scale synoptic systems. Then according to the coastline orientation, if the southeast wind at the TJ station and south and southwest winds at the QHD station occurred at approximately 11:00 LT, and the northwest wind started to blow at approximately 20:00 LT, then this type of circulation was supposed to be a sea-land circulation. The prevailing southeast wind at the TJ station and the south and southwest wind at the QHD station were regarded as sea breezes.

Comment 4:
LINE 326-335, more evidences should be given to support the statement that the movement of sea-breeze suppress the MLH at QHD site in summer. The TJ site also locates in the coastal regions, why the diurnal patterns and seasonal variations of MLH are quite different?
Response 4:
Thank you for your suggestion. Here, we re-created the monthly diurnal wind vectors as shown below in Fig.1. We can see that the sea breeze usually started at midday (approximately 11:00 LT) and prevailed during daytime at the QHD station in spring and summer (Fig. 1d). The sea breeze usually brings a cold and stable air mass from the sea to the coastal region. Under the influence of the abrupt change of aerodynamic roughness and temperature between the land and sea surfaces, a TIBL will form in the coastal areas. Then, the local mixing layer will be replaced by the TIBL. Under the influence of warm air on land, the sea air advects downwind and warms, leading to a weak temperature difference between the air and the ground. In consequence, the TIBL warms less rapidly due to the decreased heat flux at the ground, and the rise rate is reduced. In addition, since the TIBL deepens with distance downwind and usually can not extend all the way to the top of the intruding marine air, the remaining cool marine air above the TIBL will hinder the TIBL vertical development (Stull, 1988; Sicard et al., 2006). As a result, the MLH at the QHD station was lower than other stations from April to September. Since the south-southwesterly wind impacts are enhanced in summer due to the weak synoptic systems, a frequent occurrence of the TIBL resulted in the lowest MLH at the QHD station in summer. As a result, the MLH at the coastal region was affected by the TIBL, not the sea breeze, and the TIBL impact will be impaired with distance inland (Stull, 1988). Since the TJ station was approximately 50 km out to sea, the TIBL will not extend inland so far, and the MLH in TJ had no influence from the TIBL, leading to the same MLH variation with those inland sites (Beijing (BJ) and Shijiazhuang (SJZ)). The relevant contents were modified in section 4.1 in our revised manuscript.

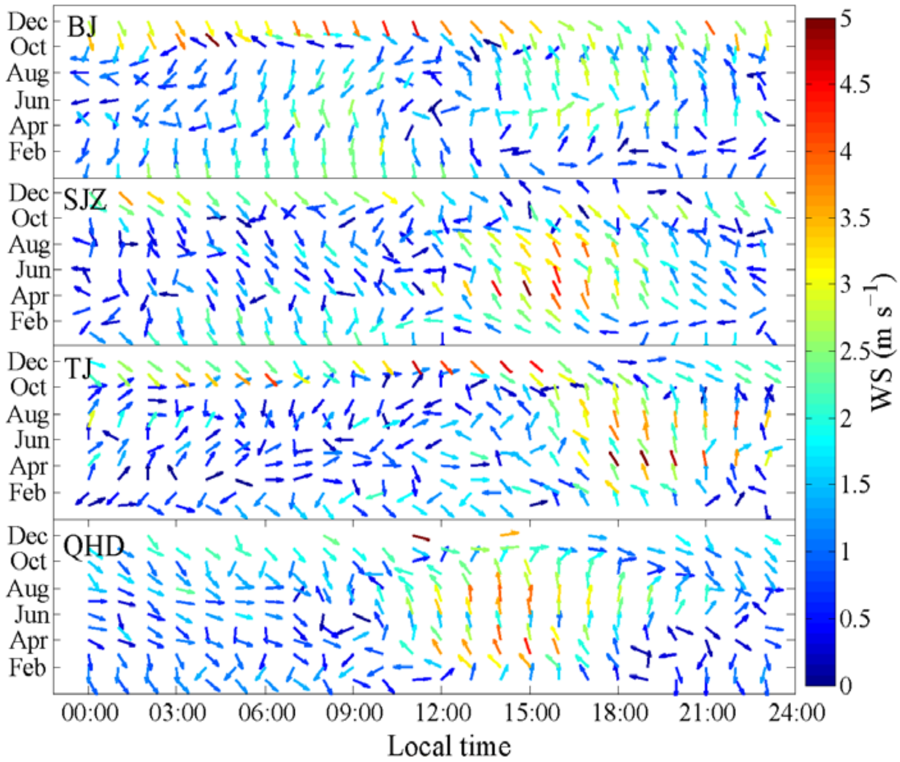

Fig. 1 Monthly variations of prevailing wind at the BJ, SJZ, TJ and QHD stations from December 2013 to November 2014.

Comment 5:

LINE 362-364, the buoyancy fluxes are determined by the surface sensible heat fluxes, not the net radiations. The statements here are inaccurate.

Response 5:

Thank you for your suggestion. The sensible heat fluxes data were not available, so we used net radiation for the analysis. Considering your suggestion, the net radiation analysis was replaced by gradient Richardson number (*Ri*) studies, and *Ri* is an index that can evaluate the turbulent stability from both the perspectives of thermal and mechanism forces. Then, the low MLH in southern Hebei mainly resulted from stable turbulent stratification (Fig.2). Relevant contents were modified in section 4.2 in the revised manuscript.

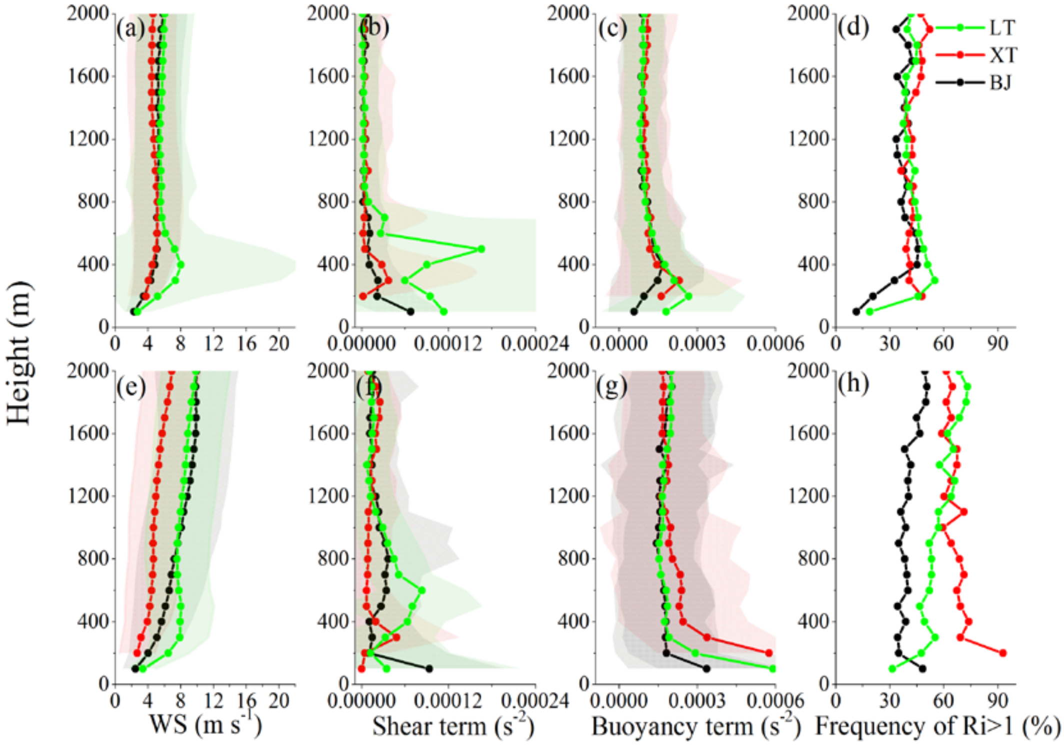

Fig.2 Vertical profiles of (a, e) the horizontal WS, (b, f) the shear term, (c, g) the buoyancy term and (d, h) the percentage of *Ri*>1 at the BJ, XT and LT stations in summer (upper panel) and winter (lower panel).

Comment 6:

LINE 371-375, before using the sounding data of XT as a replacement of SJZ, the data consistency must be examined and presented, since there are90 km between these two sites. At least, the general characteristics of MLH at SJZ at 08:00 and 20:00 LT should be well reflected by the sounding data at XT. The data consistency also should be check between the LT site and QHD site.

Response 6:

Thank you for your suggestion. Since we did not have sounding data at the SJZ and QHD stations, we used the reanalysis data to perform the examination instead. The reanalysis data were downloaded from the ECMWF website (http://apps.ecmwf.int/datasets/data/interim-full-mnth/levtype=pl/). Using the wind speed as an example, comparisons of the wind speed between the Xingtai (XT) and SJZ stations and the Laoting (LT) and QHD stations are shown in Fig. 3. The wind speed between the XT and SJZ stations, and the LT and QHD stations were highly correlated, respectively, which indicated that the sounding data in the SJZ and QHD stations could be replaced by data in the XT and LT stations, respectively.

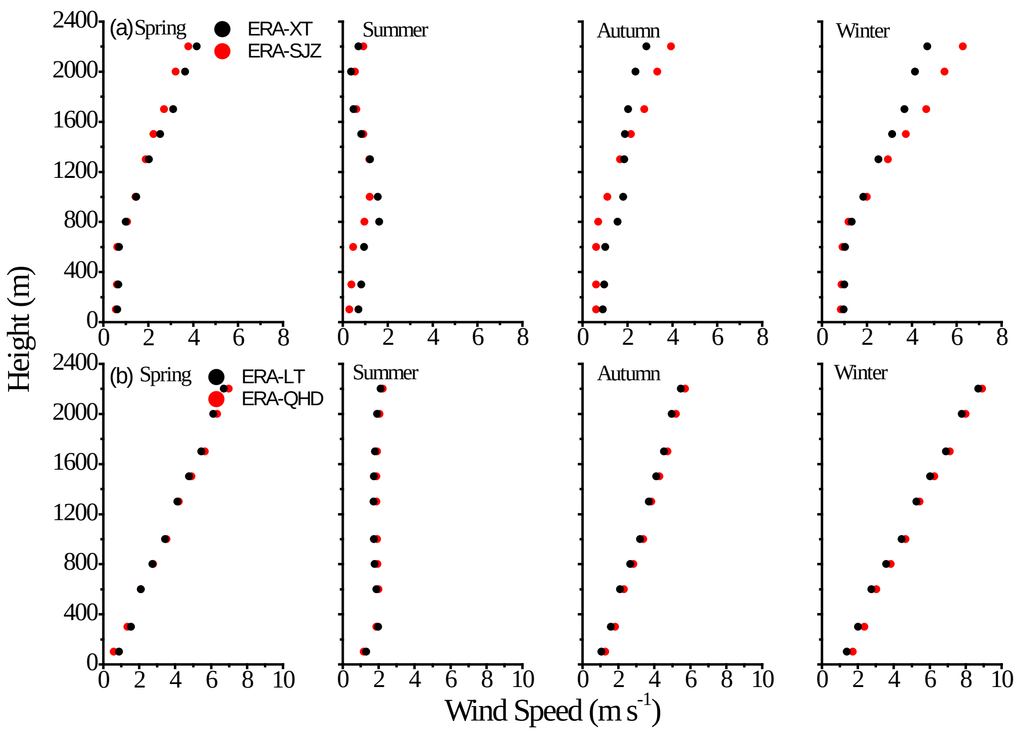

Fig. 3 Comparisons of seasonal wind speed profiles between the (a) XT and SJZ stations and the (b) LT and QHD stations with reanalysis data.

Comment 7:

As shown in Fig. 7, the profiles at XT are almost the same in different season and different moment, which is different from the profiles of other sites. The prevailing wind speed and direction are different in different season, why the profiles are almost the same? The error-bar of the profiles should also be given. In spring and summer, at 20:00 LT there are lots of fluctuations in the profiles at LT, why? Do the terrains play a role in the profiles in different regions?

Response 7:

Although the prevailing wind speed and direction at the XT station were different in different moments and seasons, the vertical variation of each wind speed profile changed slightly. Since the wind shear was defined as the degree of wind speed and direction variation between the upper layer and the lower layer (wind shear = $\sqrt{\left(\frac{\Delta \overline{u}}{\Delta z}\right)^2 + \left(\frac{\Delta \overline{v}}{\Delta z}\right)^2}$), the almost consistent wind shear profiles in different seasons and different moments indicated a relatively stable atmospheric stratification. Similarly, the stronger variation and higher value of wind shear in the vertical direction at the BJ station suggested a relatively unstable atmospheric stratification, which was probably due to the frequent passage of cold air masses. Fig. 1 shows that the sea breeze changed to land breeze at approximately 20:00 LT; thus, the fluctuations in the profiles at LT could be attributed to the transitory stages of sea-land breeze alternation. Therefore, the terrains certainly play a role in the wind shear profiles in different regions. To further interpret the reasons for low MLH at southern Hebei, we included an analysis of gradient Richardson number (*Ri*) profiles at the BJ, XT and LT stations in the revised manuscript and the wind shear study was replaced by the study of shear term ($\left(\frac{\Delta \bar{u}}{\Delta z}\right)^2 + \left(\frac{\Delta \bar{v}}{\Delta z}\right)^2$). Since the comparison results at 08:00 LT and 20:00 LT made no difference, we combined the sounding profiles at 08:00 LT and 20:00 LT to make our paper concise and easily understood (Fig. 2). Then, the low MLH in southern Hebei mainly resulted from stable turbulent stratification

Comment 8:
LINE 390-392, the authors merely presented the profiles at 20:00 LT, which cannot support the statement "during the whole night". More evidences should be given.
Response 8:
Thank you for your suggestion. In our revised manuscript, the meteorological profiles were averaged over 08:00 LT and 20:00 LT, and the shear term and buoyancy term profiles were compared between southern Hebei and the northern NCP (Fig. 2). The wind shear term in southern Hebei was lower than that in the northern NCP within 0-1200 m in spring, autumn and winter, while the buoyancy term was on the opposite, leading to a conclusion that the low MLH in southern Hebei resulted from stable turbulent stratification. In summer, this discrepancy was largely decreased and the MLHs were consistent between these two areas. The relevant contents were modified in section 4.2 in the revised manuscript.

Comment 9:
LINE 404-405, please give evidences to support the statement "the front usually does not reach southern Hebei".
Comment 10:
LINE 406-408, please give evidences to support the statement "the lessened effects of the front system and strong turbulent exchange will lead to less wind shear contrast in the vertical direction between southern Hebei and the northern NCP."
Response 9 and 10:
Thank you for your suggestion and we are sorry for our misrepresentation. Although haze evolution in the NCP area is usually regionally consistent, the pollution intensity varies in different regions, which will be partially attributed to the impact of different positions of weather systems. The NCP region is usually influenced by the continental high in the spring, autumn and winter in the lower troposphere. When the high pressure is relatively weak, the northern and southern areas are usually located in front and to the south of the system, respectively. Thus, the weak cold and clean air may be partially responsible for the lighter pollution degree in the northern NCP areas (Su et al., 2004). Meanwhile, the cold front caused by the cold air flow over the northern NCP will enhance the shear term. In summer, due to the northward lift and westward intrusion of the subtropical high on the NCP, the diminished effect of the weak cold air on the northern NCP accompanied with strong solar radiation and turbulent activities will lead to less shear term contrast in the vertical direction between southern Hebei and the northern NCP. Based on this, we have made

modifications in section 4.2 in our revised manuscript.

Comment 11:
LINE 410-419, the authors attribute the high PM concentration in SJZ to the low MLH. It is inaccurate, the different anthropogenic emissions of pollutants in SJZ and BJ should be considered.

Response 11:
Thank you for your suggestion. Since the particle has direct emission sources and secondary sources, the direct emissions distribution cannot represent the total emissions contribution to the particle concentration. The near-ground $PM_{2.5}$ concentration could represent the particle concentrations at the ground, but considering that the lifetime of a particle is much longer than that of trace gases, the particle concentrations are nearly uniform in the mixing layer because of the strong vertical mixing. Therefore, near-ground $PM_{2.5}$ concentrations cannot be used to evaluate the emissions influences between different regions if the mixing layer heights are different. AOD, which represents the aerosol column concentration, is a much better indicator for the emissions difference. In the revised manuscript, we checked the AOD distribution in the NCP to evaluate the emissions effect. The AOD data were retrieved with the dark target algorithm from the Moderate Resolution Imaging Spectra-radiometer (MODIS) aerosol products on board the NASA EOS (Earth observing system) Terra satellite. As shown in Fig. 4, the averaged AOD value at southern Hebei (SJZ, Handan (HD) and Xingtai (XT)) was 1.2 times higher than the AOD at the northern NCP (BJ and TJ) region, while the near-ground $PM_{2.5}$ concentration in southern Hebei was 1.5 times higher than that in the northern NCP. If the difference of AOD represents the emissions discrepancy, the remaining differences of the $PM_{2.5}$ concentration may be induced by the meteorology. In other words, except for the emissions effect, the meteorological conditions also play an important role in pollutant contrast between these two areas. Relevant contents were also modified in section 4.3 in our revised manuscript.

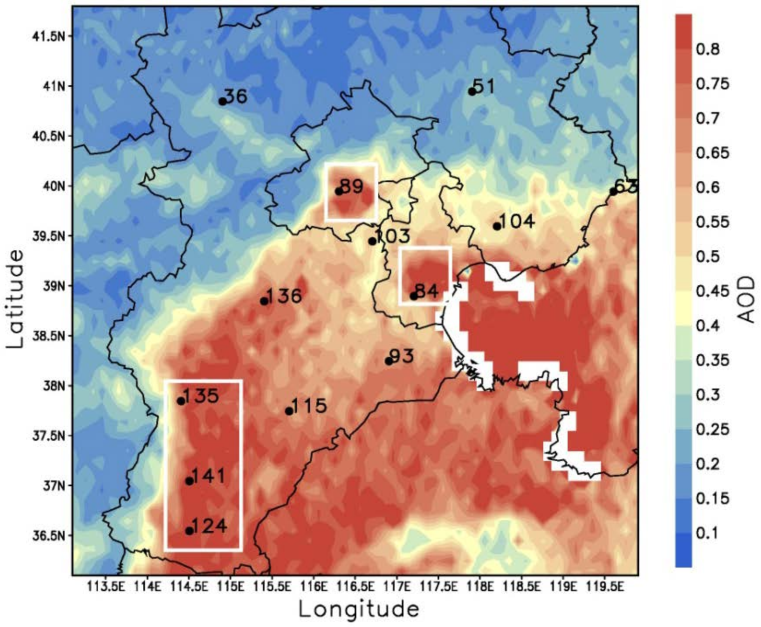

Fig. 4 Distribution of AOD from December 2013 to November 2014 in the NCP. The $PM_{2.5}$ concentrations of the 13 observation sites were also marked beside each station. Major sites in the northern NCP (BJ and TJ) and southern Hebei (SJZ, XT and HD) are enclosed by white rectangles.

Comment 12:
LINE 420-422, although the RH can affect the visibility, it cannot significantly affect the aerosol concentration. Is there any direct physical connections between the high RH conditions and high aerosol concentration?
Response 12:
The RH can not only affect the visibility but also the aerosol concentrations. The direct physical mechanism is the fine particle's hygroscopic growth and the RH has a positive correlation with the fine particle's number and mass concentrations (Hu et al., 2006; Liu et al., 2011; Seinfeld et al., 1998).

Comment 13:
LINE 426-427, "temperature is the main factor in new particle formation," any evidences to support this statement in NCP.
Response 13:
Thank you for your suggestion, and we apologize for this inappropriate illustration. Actually, the temperature has impact on the particles physicochemical reaction rate. The particles' nucleation and other secondary transformation processes are most efficient in a relatively high temperature and RH. If the temperature was lower than the ideal value, the aerosol's secondary transformation processes would be less effective (Seinfeld et al., 1998).

Comment 14:
LINE 437-440, the RH in SJZ is higher than that in TJ (closer to sea), why?
Response 14:
Thank you for your suggestion. The seasonal distributions of near-ground RH from December 2013 to November 2014 in the NCP are depicted in Fig. 5. It is clear that southern Hebei had higher RH values than the northern NCP. The RH distribution was not only related to the distance from the sea but also to the flow fields and synoptic systems. This might resulted from the frequent passage of the Siberian High in the northern NCP, especially in spring and winter. In spring, when frequent sand storms occur, a dry air mass is brought to the northern NCP; thus, the RH in the northern NCP was far less than that in southern Hebei (Fig. 5a). Meanwhile, under the impact of the Siberian High, a frequent weak northwest flow from Inner Mongolia will bring cold and dry air to the northern NCP in winter and autumn, and the north flow was too weak to reach southern Hebei (Su et al., 2004), which will lead to a lower RH in the northern NCP (Fig. 5c and 5d). Additionally, the higher RH in southern Hebei could also be affected by the subtropical high in summer (wet southeast flow from the Yellow Sea) (Fig. 5b).

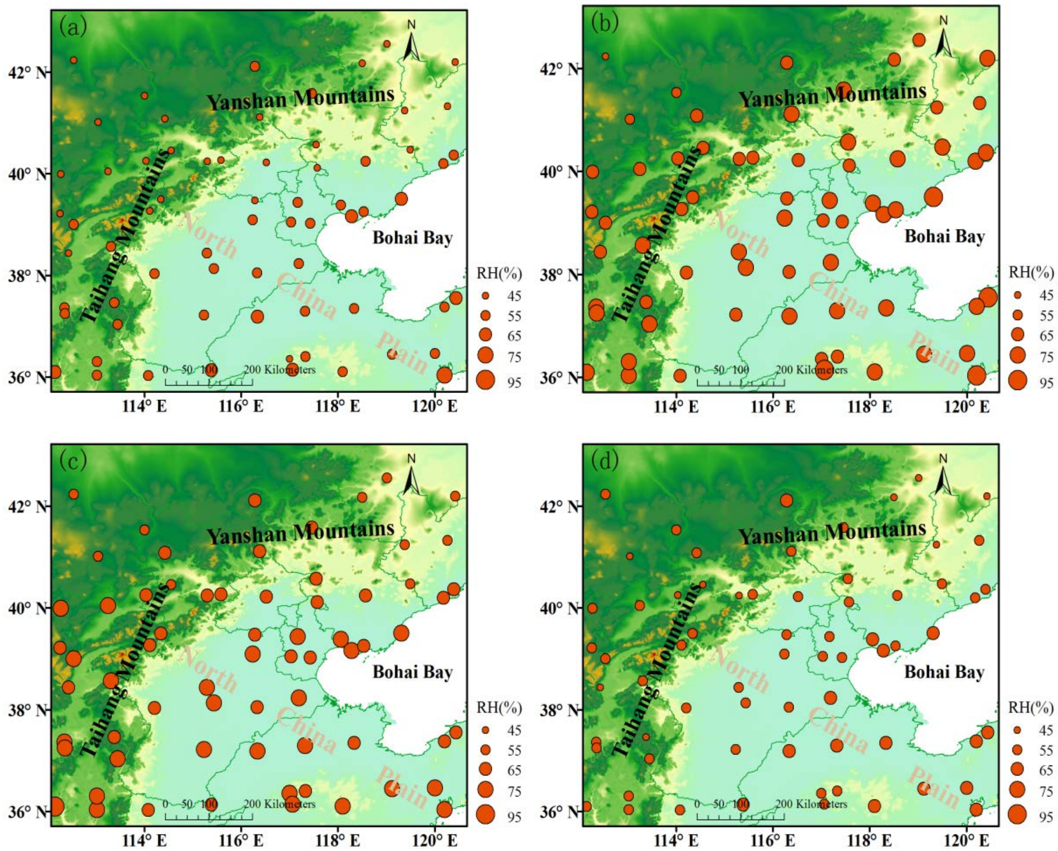

Fig. 5 Distributions of seasonal averaged RH in the NCP from December 2013 to November 2014: (a) spring, (b) summer, (c) autumn and (d) winter.

Comment 15:

Section 4.2.1, the authors attribute the higher PM in SJZ to new particle formation, which is quite complex and cannot be understood merely by the surface temperature and RH. And the direct emissions of pollutants should be considered.

Response 15:

Thank you for your suggestion. Since the particle has direct emissions sources and secondary sources, the distribution of direct emissions cannot represent the total contribution of emissions to the particle concentration. The near-ground $PM_{2.5}$ concentration could represent the particle concentrations at the ground, but considering that the particle lifetime is much longer than that of trace gases, the particle concentrations are nearly uniform in the mixing layer because of strong vertical mixing. Therefore, near-ground $PM_{2.5}$ concentrations cannot be used to evaluate the emissions influences between different regions if the mixing layer heights are different. AOD, which represents the aerosol column concentration, is a much better indicator for the emissions difference. As shown in Fig. 4, the averaged AOD value at southern Hebei (SJZ, HD and XT) was 1.2 times higher than the AOD at the northern NCP (BJ and TJ) region, while the near-ground $PM_{2.5}$ concentration in southern Hebei was 1.5 times higher than that in the northern NCP. If the difference of AOD represents the emissions discrepancy, the remaining differences of the $PM_{2.5}$ concentration may be induced by the meteorology. In other words, except for the emissions effect, the meteorological conditions also play an important role in pollutant contrast between these two areas. The lower MLH combined with higher RH and weaker wind speed contributed to the heavier haze in southern Hebei. Relevant contents were also modified in section 4.3 in our revised manuscript.

Comment 16:
LINE 470-473, “it was considered reasonable to regard the sounding data of WS as a climatological constant”, during a day, the WS within ML would change due to the momentum exchanges between the ML and free troposphere. The WS cannot be considered as a constant. As illustrated in Fig. S2, there are differences in profiles at 08:00 and 20:00 LT. The error-bar of wind speed should be given.

Response 16:
Thank you for your suggestion, and we apologize for this inaccurate expression. The wind speed in our study was supposed to be a climatological feature, not a climate constant. Additionally, the wind speeds at 08:00 LT and 20:00 LT were used to approximately calculate the ventilation coefficient. Although it will be better to include the sounding data at noon, this is the best choice at present due to the confined acquired data. Relevant contents were supplemented in the conclusion section to explain the uncertainties of our study.

References:

Hu, M., S. Liu, Z. Wu, J. Zhang, Y. Zhao, W. Birgit, and W. Alfred: Effects of high temperature, high relative humidity and rain process on particle size distributions in the summer of Beijing, Environ. Sci., 27(11), 2006.

Liu, Z., Y. Sun, L. Li and Y. Wang: Particle mass concentrations and size distribution during and after the Beijing Olympic Games, Environ. Sci., 32(4), doi:10.13227/j.hjkx.2011.04.015, 2011.

Seinfeld, J. and S. Pandis: Atmospheric Chemistry and Physics: From Air Pollution to Climate Change, New York: John Wiley and Sons, 1998.

Sicard, M., C. Pérez, F. Rocadenbosch, J. Baldasano, and D. García-Vizcaino,: Mixed-Layer Depth Determination in the Barcelona Coastal Area From Regular Lidar Measurements: Methods, Results and Limitations. Boundary-Layer Meteorology 119, 135-157, 2006.

Stull, R.: An Introduction to Boundary Layer Meteorology, Kluwer Academic Publishers, Dordrecht, 1988.

Su, F., M. Yang, J. Zhong, and Z. Zhang: The effects of synoptic type on regional atmospheric contamination in North Chian, Res. Of Environ. Sci., 17(3), doi:10.13198/j.res.2004.03.18.sufq.006, 2004.

Mixing layer height on the North China Plain and meteorological evidence of serious air pollution in southern Hebei

Xiaowan Zhu[1,23], Guiqian Tang[1,~~2~~*], Jianping Guo[34], Bo Hu[1], Tao Song[1], Lili Wang[1], Jinyuan Xin[1], Wenkang Gao[1], Christoph Münkel[45], Klaus Schäfer[56], Xin Li[1,67], and Yuesi Wang[1]

[1]State Key Laboratory of Atmospheric Boundary Layer Physics and Atmospheric Chemistry (LAPC), Institute of Atmospheric Physics, Chinese Academy of Sciences, Beijing 100029, China
~~[2]Center for Excellence in Regional Atmospheric Environment, Institute of Urban Environment, Chinese Academy of Sciences, Xiamen 361021, China~~
[23]University of Chinese Academy of Sciences, Beijing 10049, China
[34]State Key Laboratory of Severe Weather & Key Laboratory of Atmospheric Chemistry of CMA, Chinese Academy of Meteorological Sciences, Beijing 100081, China
[45]Vaisala GmbH, 22607 Hamburg, Germany
[56]Atmospheric Science College, Chengdu University of Information Technology (CUIT), Chengdu 610225, China
[67]Beijing Municipal Committee of China Association for Promoting Democracy, Beijing 100035, China

Correspondence to: G. Tang (tgq@dq.cern.ac.cn)

Abstract

To investigate the spatiotemporal variability of ~~regional~~ the mixing layer height (MLH) on the North China Plain (NCP), multi-site and long-term observations of the MLH with ceilometers at three inland stations (~~[e.g.,~~ Beijing (BJ), Shijiazhuang (SJZ) and ~~,~~ Tianjin (TJ)~~]~~) and one coastal site (~~[e.g.,~~ Qinhuangdao ~~(QHD)]~~) were conducted from 16 October 2013 to 15 July 2015. The MLH of~~at~~ the inland stations i~~o~~n the NCP were highest in summer and lowest in winter, while the MLH o~~i~~n the coastal area of Bohai was lowest in summer and highest in spring. ~~The regional MLH developed the earliest in summer (at approximately 7:00 LT) and reached the highest growth rates (164.5 m h^{-1}) at approximately 11:00 LT, while in winter, the regional MLH developed much later (at approximately 9:00 LT), with the maximum growth rates (101.8 m h^{-1}) occurring at 11:00 LT.~~ As a typical site in southern Hebei, the annual mean of the MLH at SJZ was 464±183 m, which was 15.0 % and 21.9 % lower than that at the BJ (594±183 m) and TJ (546±197 m) stations, respectively. Investigation of ~~radiation and~~ the ~~wind~~ shear term and buoyancy term in~~at~~ the NCP revealed that these two parameters in southern Hebei were 2.8 times lower and 1.5 times higher than that in northern NCP within 0-1200 m in winter, respectively, leading to a 1.9~~the net radiation was almost consistent on a regional scale, and the lower MLH in southern Hebei was mainly due to the 1.9-2.8~~-fold higher ~~intensity of wind shear~~frequency of

the Gradient Richardson number >1 in southern Hebei compared to ~~than on~~ the northern NCP ~~than in southern Hebei~~ ~~at an altitude of 300-1700 m~~. Furthermore, combined with aerosol optical depth and $PM_{2.5}$ observations, we found that the pollutant column concentration contrast (1.2 times) between these two areas was far less than the near-ground $PM_{2.5}$ concentration contrast (1.5 times). Through analysis of the ventilation coefficient ~~and the relative humidity~~ in ~~southern Hebei were 1.1-2.1 times smaller and 13.2-22.1 % higher than that on~~ the ~~northern~~ NCP, ~~–~~ the near-ground heavy pollution in southern Hebei mainly resulted from the lower MLH and wind speed.~~respectively.~~ Therefore~~As a result~~, ~~severe haze pollution occurred much more readily in southern Hebei and the annual means of near-ground $PM_{2.5}$ concentrations were almost 1.3 times higher than those of the northern areas,~~. ~~d~~Due to the importance of unfavorable weather conditions, ~~industrial capacity should be reduced in southern Hebei,~~ heavily polluting enterprises should be relocated, and strong emission reduction measures are required to improve the air quality in southern Hebei.

带格式的：下标

带格式的：下标

1. Introduction

The convective boundary layer is the region where turbulence is fully developed. The height of the interface where turbulence is discontinuous is usually referred to as the mixing layer height (MLH) (Stull, 1988). The mixing layer is regarded as the link between the near-surface and free atmosphere, and the MLH is one of the major factors affecting the atmospheric dissipation ability, which determines both the volume into which ground-emitted pollutants can disperse, as well as the convective time scales within the mixing layer (Seidel et al., 2010). In addition, continuous MLH observations will be of great importance for the improvement of boundary layer parameterization schemes and for the promotion of meteorological model accuracy.

Conventionally, the MLH is usually estimated from radiosonde profiles (Seidel et al., 2010). Although meteorological radiosonde observations can provide high-quality data, they are not suitable for continuous fine-resolution MLH retrievals due to their high cost and limited observation intervals (Seibert et al., 2000). As the most advanced method of MLH detection, remote sensing techniques based on the profile measurements from ground-based instruments such as sodar, radar, or lidar that have the unique vertically resolved observational capability are becoming increasingly popular (Beyrich, 1997; Chen et al., 2001; He et al., 2005). Because sound waves can be easily attenuated in the atmosphere, the vertical range of sodar is generally limited to within 1000 m. However, the optical remote sensing techniques can provide higher height ranges (at least several kilometers). The single-lens ceilometers developed by Vaisala have been widely used in a variety of MLH studies (~~e.g.,~~ Alexander et al., 2017; Emeis et al., 2004, 2009, 2011; ~~Emeis et al., 2009; Emeis et al., 2011;~~ Eresmaa et al., 2006; Münkel et al., 2004, 2007~~2006~~; Muñoz and Undurraga, 2010; ~~Munkel and Rasanen, 2004;~~ Schween et al., 2014; Sokół et al., 2014; Tang et al., 2015, 2016; Wagner et al., 2006, 2015~~; Tang et al., 2015b~~). Compared with other remote sensing instruments, this type of lidar has special features favorable for long-term and multi-station observations (Emeis et al., 2009; Wiegner et al., 2014; Tang et al., 2016), including the low-power system, the eye-safe operation within a near infrared laser band, and the low cost and ease of maintenance during any weather conditions (excluding rainy, strong windy or sandstorm weather conditions) with only regular window cleaning required (Emeis et al., 2004; Tang et al., 2016).

The North China Plain (NCP) region is the political, economic and cultural center of China. With the rapid economic development, energy use has increased substantially, resulting in frequent air pollution episodes (~~e.g.,~~ Guo et al., 2011; Li et al., 2013; Liu et al., 2016; Tang et al., ~~2015a~~2017; Wang et al., 2014; Wang et al., 2013a; Xu et al., 2016; Zhang et al., 2014). The haze pollution has had an adverse impact on human health (Tang et al., 2017a) and has aroused a great deal of concern (Tang et al., 2009; Ji et al., 2012; Zhang et al., 2015a). To achieve the integrated ~~of~~ development of the Jing-Jin-Ji region, readjustment of the regional industrial structure and layout is imperative. To this end, the industrial capacity of heavily polluting enterprises in the areas with unfavorable weather conditions should be reduced, and these heavily polluting enterprises should be removed to improve the air quality. For the remaining enterprises, the industrial air pollutant emissions structure should be changed, and strong emission reduction measures must be implemented. Although the government has carried out some strategies for joint prevention and control, with the less well-understood distributions of regional weather condition ~~status~~ on the NCP, how and where to adjust the industrial structures on the NCP are questions in pressing need of answers. As one of the key factors influencing the regional heavy haze pollution (Tang et al., 2012, 2016, 2017b; Quan et al., 2013; Hu et al., 2014; ~~Tang et al., 2016;~~ Zhu et al., 2016; ~~Tang et al., 2017b;~~ Zhang et al., 2016a), the MLH to some extent represents the atmospheric environmental capacity, and the regional distribution and variation of MLH on~~in~~ the NCP can offer a scientific basis for regional industrial distribution readjustment, which will be of great importance for regional haze management.

Nevertheless, due to the scarcity of MLH observations on the NCP, reliable and explicit characteristics of MLH on the NCP remain unknown. Tang et al. (2016) utilized the long-term observation data of MLH from ceilometers to analyze the characteristics of MLH variations in Beijing (BJ) and verified the reliability of ceilometers. The results demonstrated that MLH in BJ was high in spring and summer and low in autumn and winter with two transition months in February and September. A multi-station analysis of MLH ~~in~~ on the NCP region was conducted in February 2014, and the characteristics of high MLH at coastal stations and low MLH at southwest piedmont stations were reported (Li et al., 2015). Miao et al. (2015) modeled the seasonal variations of MLH on the NCP and discovered that the MLH was high in spring due to the strong mechanical forcing and low in winter as a result of the strong thermodynamic stability in the near-surface layer. The mountain-plain breeze and the sea breeze circulations played an important role in the mixing layer process when the background synoptic patterns were weak in summer and autumn (Tang et al., 2016; Wei et al., 2017).

~~However, the regional MLH simulation analysis is incomplete without verification with long-term measured MLH data.~~ To overcome previous studies' deficiencies, our study first conducted a 22-month~~s~~ (from 16 October 2013 to 15 July 2015) observation of MLH with ceilometers on the NCP. The observation stations included three inland stations ~~[e.g., ~~(BJ, Shijiazhuang (SJZ) and Tianjin (TJ)~~]~~) and one coastal site ~~[e.g., ~~(Qinhuangdao (QHD))~~]~~. First, we will describe the spatial and temporal distribution of MLH on the NCP. Subsequently, reasons for spatial difference of MLH ~~differences ~~on the NCP will be explained in the discussion section. Finally, ~~the ~~the meteorological evidence of serious air pollution in southern Hebei will be studied ~~weather conditions on the NCP are described to provide a scientific basis for regional industrial structure readjustment~~.

2 Data and methods

2.1 Sites

To study the ~~regional ~~MLH characteristics ~~in ~~on the NCP~~ region~~, observations with ceilometers were conducted at the BJ, SJZ, TJ and QHD stations from 16 October 2013 to 15 July 2015 (Fig. 1 and Table S1). The SJZ, TJ and QHD sites were set around Beijing in the ~~east~~southwest, southeast and ~~southwest ~~east directions, respectively. The BJ station was at the base of the Taihang and Yanshan Mountains on the northern NCP. The MLH observation site was built in the courtyard of the Institute of Atmospheric Physics, Chinese Academy of Sciences (116.32° E, 39.90° N). SJZ was near the Taihang Mountain in southern Hebei; the location was in the Hebei University of Economics (114.26° E, 38.03° N). The TJ site was set in the courtyard of the Tianjin Meteorological Bureau, which was located south of the urban area, with a geographic location of 117.20° E, 39.13° N. The QHD station was an eastern coastal site of Bohai Bay, which was set up in the Environmental Management College of China (119.57° E, 39.95° N), and the surrounding areas are mostly residential buildings with no high structures. Since the TJ site was approximately 50 km away from the coast and the QHD station was only 2 km, the TJ station, by contrast, was supposed to be an inland station.

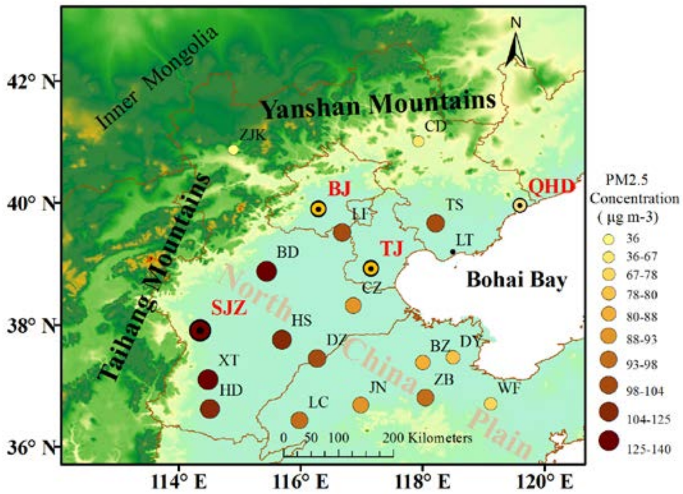

Fig. 1~~.~~ Locations of the ceilometers observation sites (BJ, SJZ, TJ and QHD) are marked with red and bold abbreviations; other $PM_{2.5}$ observation sites (ZJK, CD, LF,

TS, CZ, BD, HS, XT, HD, DZ, LC, JN, BZ, DY, ZB and WF) and the sounding observation sites (BJ, LT and XT) are marked on the map with black abbreviations. The size and color of the circular mark are representatives of the annual mean of near-ground $PM_{2.5}$ concentration; the larger and darker the circle is, the greater the concentration iss.

Table 1. Specific information of the observation sites on the NCP.

Cityname	Abbreviation	Province or municipality	Longitude	Latitude
Beijing[a,b,c]	BJ	Beijing	116.32° E	39.90° N
Tianjin[a,b]	TJ	Tianjin	117.20° E	39.13° N
Shijiazhuang[a,b]	SJZ	Hebei	114.26° E	38.03° N
Langfang[a]	LF	Hebei	116.70° E	39.53° N
Tangshan[a]	TS	Hebei	118.02° E	39.68° N
Qinhuangdao[a,b]	QHD	Hebei	119.57° E	39.95° N
Zhangjiakou[a]	ZJK	Hebei	114.92° E	40.90° N
Chengde[a]	CD	Hebei	117.89° E	40.97° N
Laoting[b,c]	LT	Hebei	118.90° E	39.31° N
Cangzhou[a]	CZ	Hebei	116.83° E	38.33° N
Baoding[a]	BD	Hebei	115.48° E	38.85° N
Hengshui[a]	HS	Hebei	115.72° E	37.72° N
Xingtai[b,c]	XT	Hebei	114.48° E	37.05° N
Handan[a]	HD	Hebei	114.47° E	36.60° N
Dezhou[a]	DZ	Shandong	116.29° E	37.45° N
Liaocheng[a]	LC	Shandong	115.97° E	36.45° N
Jinan[a]	JN	Shandong	116.98° E	36.67° N
Binzhou[a]	BZ	Shandong	118.02° E	37.22° N
Dongying[a]	DY	Shandong	118.49° E	37.46° N
Zibo[a]	ZB	Shandong	118.05° E	36.78° N
Weifang[a]	WF	Shandong	119.06° E	36.68° N

[b]Near-ground $PM_{2.5}$ concentration sites.

[a]Ceilometer observation sites.

带格式的: 非上标/ 下标

[a]Ceilometer observation sites.

[b]Near-ground $PM_{2.5}$ concentration sites.

[c]Radiosonde observation sites.

2.2 Measurement of MLH

The instrument used to measure the MLH at the four stations was an enhanced single-lens ceilometer (Vaisala, Finland), which utilized the strobe laser lidar (laser detection and range measurement) technique (910 nm) to measure the attenuated backscattering coefficient profiles. As large differences existed in the aerosol concentrations between the mixing layer and the free atmosphere, the MLH can be determined from the vertical attenuated backscattering coefficient (β) gradient, whereby a strong, sudden change in the negative gradient (-dβ/dx) can indicate the MLH. In the present study, the Vaisala software product BL-VIEW was utilized to calculate the MLH by determining the location of the maximum $|-d\beta/dx|$ ~~$-d\beta/dx$~~ in the attenuated backscattering coefficient. To strengthen the echo signals and reduce the detection noise, spatial and temporal averaging should be conducted before the gradient method is used to calculate the MLH. The BL-VIEW software was utilized with temporal smoothing of 1200 s and vertical distance smoothing of 240 m. The instrument installed at the BJ station was a CL31 ceilometer and the CL51 ceilometers were used at the SJZ, TJ and QHD stations. Some of the properties of these two instruments are listed in Table 1~~2~~, and basic technical descriptions can be found in Münkel et al. (2007) and Tang et al. (2015).

To ensure the consistency of the MLH measurements~~d~~ with the two different ~~versions of~~ ceilometer versions~~s~~, before we set up the ceilometer observation networks ~~at different stations~~in the NCP, we made a comparison of the MLHs observed by CL31 and CL51 at BJ from October 1 to October 8, 2013 (Fig. S1). The MLH observed by CL~~-~~31 was highly ~~correlated with~~relevant to those observed by ~~each of~~ the ~~three~~ CL51 ceilometers, with ~~relative~~ correlation coefficients (R) of 0.~~92~~86-0.92~~, 0.86 and 0.92~~. Therefore, the impact of version discrepancy on the MLH measurement can be neglected.

Since the ceilometers can reflect rainy conditions and the precipitation will influence the MLH retrieval, the precipitation data were excluded. In addition, a previous study has compared MLH measurements retrieved from ceilometers and sounding data (Tang et al., 2016). T~~, t~~he results revealed that the ceilometers underestimates the MLH under neutral conditions caused by strong winds and overestimate the MLH when sand storms occur. Therefore, data points for these three special weather conditions were eliminated manually. The criterion to exclude these data points is as follows: (a) precipitation, i.e., a cloud base lower than 4000 m and the attenuated backscattering coefficient of at least 2×10^{-6} $m^{-1}sr^{-1}$ within 0 m and the cloud base, (b) sandstorm, i.e., the ratio of $PM_{2.5}$ to PM_{10} suddenly decreased to 30 % or lower and the PM_{10} concentration was higher than 500 μg m^{-3}, and (c) strong winds, i.e., a sudden change in temperature and wind speed (WS) when cold fronts passed by (Muñoz and Undurraga, 2010; Tang et al., 2016; Van der Kamp and McKendry, 2010).

带格式的：不调整西文与中文之间的空格，不调整中文和数字之间的空格
带格式的：字体颜色：红色
带格式的：字体颜色：红色
带格式的：字体颜色：红色
带格式的：字体颜色：红色
带格式的：字体颜色：红色

Table 1~~2.~~ Instrument properties of CL31 and CL51

Parameter	CL31	CL51
Detection range (km)	7.7	13.0
Wavelength (nm)	910	910
Report period (s)	2-120	6-120
Report accuracy (m)	5~~m~~	10~~m~~
Peak power (W)	310	310

2.3 Other data

The hourly data of near-ground relative humidity (RH) and ~~,~~ temperature (T) ~~,~~

near-ground wind speed (WS) and direction at the BJ, SJZ, TJ and QHD stationsin the NCP region were obtained from the China Meteorological Administration (http://www.weather.com.cn/weather/101010100.shtml/). Hourly net (0.2-100 μ m) radiation data at the BJ, TJ and SJZ sites were observed using a net radiometer (NR Lite2, Kipp & Zonen, Netherlands), detailed information is included in Hu et al., (2012). To study the reason for the MLH difference between the northern NCP and southern Hebei, meteorological sounding data were included in this paper. The data were provided by the upgraded radiosonde network of China, where the GTS1 digital electronic radiosonde was required to be operationally launched twice per day at 08:00 LT and 20:00 LT by the China Meteorological Administration (Guo et al., 2016). Considering the deficiency of sounding data at the SJZ and QHD stations, data from the Xingtai (XT) and Laoting (LT)XT and LT stations were used instead after a consistency test with the reanalysis data (Fig. S2). Because the SJZ and QHD stations are missing radio sounding data, sounding data from the XT and LT stations were used instead. The reanalysis data at these four sites were downloaded from the website of European Centre for Medium-Range Weather Forecasts (http://apps.ecmwf.int/datasets/data/interim-full-mnth/levtype=pl/). Sounding data of WS and direction at the BJ, XT and LT stations were provided by the upgraded radiosonde network of China, where the GTS1 digital electronic radiosonde was required to be operationally launched twice per day at 08:00 LT and 20:00 LT by the China Meteorological Administration (Guo et al., 2016).

The near-ground $PM_{2.5}$ and PM_{10} concentrations at the 20 observation sites from December 2013 to November 2014 were provided by the Ministry of Environmental Protection (http://www.zhb.gov.cn/) with a time resolution of 1 h (http://www.zhb.gov.cn/). Details for the near-ground $PM_{2.5}$ and PM_{10} observation sites are listed shown in Table S1 and Fig. 1.

The aerosol optical depth (AOD) data within the NCP region were retrieved with the dark target algorithm from the Moderate Resolution Imaging Spectra-radiometer aerosol products on board the National Aeronautics and Space Administration Earth Observing System Terra satellite from December 2013 to November 2014 (Zhang et al., 2016b) (https://ladsweb.nascom.nasa.gov/search/index.html/), then the AOD data was interpolated into 0.1°×0.1° to produce the regional distribution in the NCP.

2.4 Atmospheric stability criterion

The Gradient Richardson number (*Ri*) is usually used to estimate the atmospheric turbulent stability within the mixing layer and is defined as follows (Eq. 1):

$$Ri = \frac{\frac{g}{\bar{\theta}}\frac{\Delta\bar{\theta}}{\Delta z}}{\left(\frac{\Delta\bar{u}}{\Delta z}\right)^2+\left(\frac{\Delta\bar{v}}{\Delta z}\right)^2} \qquad (1)$$

Where Δz is the height increment over which a specific calculation of *Ri* is being made; g is the acceleration of gravity; $\bar{\theta}$ is the mean virtual potential temperature

带格式的
带格式的: 缩进: 首行缩进: 1 字符
带格式的: 字体: 小三, (国际) Times New Roman
带格式的: 字体: 小三
带格式的: 字体: 小三, (国际) Times New Roman
带格式的: 字体: 小三, (国际) Times New Roman
带格式的: 字体: Times New Roman, 小三
带格式的: 字体: Times New Roman, 小三
带格式的: 字体: Times New Roman, 小三
带格式的: 字体: Times New Roman, 小三
带格式的: 字体: 小三, (国际) Times New Roman
带格式的: 字体: Times New Roman, 小三
带格式的: 字体: 小三, (国际) Times New Roman
带格式的: 字体: Times New Roman, 小三
带格式的: 字体: 小三, (国际) Times New Roman
带格式的: 字体: 小三, (国际) Times New Roman
带格式的: 字体: 小三, (国际) Times New Roman
带格式的: 字体: Times New Roman, 小三
带格式的: 字体: 小三, (国际) Times New Roman
带格式的: 字体: Times New Roman, 小三
带格式的: 字体: 小三, (国际) Times New Roman
带格式的: 字体: 小三, (国际) Times New Roman
带格式的: 字体: (国际) Times New Roman
带格式的: 字体: (国际) Times New Roman

within that height increment; and $\Delta\bar{u}$ and $\Delta\bar{v}$ are the mean wind speeds in zonal and meridional directions within the height increment.

Using *Ri* to diagnose turbulence is a classical approach and has been covered in many textbooks on boundary-layer turbulence (Stull, 1988; Garratt, 1994). It can be interpreted as the ratio of the buoyancy term ($\frac{g}{\bar{\theta}}\frac{\Delta\bar{\theta}}{\Delta z}$) to the shear term ($\left(\frac{\Delta\bar{u}}{\Delta z}\right)^2 + \left(\frac{\Delta\bar{v}}{\Delta z}\right)^2$) in the turbulent kinetic equation. When the *Ri*>1, the turbulence was suppressed and the mixing layer development will be restrained (Stull, 1988). In our study, the frequency of *Ri*>1 was used to represent the atmospheric stability in the NCP. The larger the frequency is, the more stable turbulent stratification is.

3 Results

3.1 Frequency distribution of ~~regional~~ MLH

Since October 2013, c~~C~~ontinuous operation of the ceilometers observation network in the NCP ~~since October 2013~~ has provided 22 months of MLH data.~~,~~ ~~F~~and ~~f~~or the purpose of analyzing ~~of~~ the MLH temporal and spatial ~~variability~~ variation~~in the NCP region~~, the hourly averages of MLH for a whole year (from December 2013 to November 2014) at the BJ, SJZ, TJ and QHD stations were ~~utilized~~ chosen in the following ~~study~~sections. Hourly means of MLH under rainy, sandstorm and windy conditions were removed ~~(Muñoz and Undurraga, 2010; Tang et al., 2016; van der Kamp and McKendry, 2010)~~, resulting in data availability of 81, 89, 83 and 77 % at the BJ, SJZ, TJ and QHD stations, respectively. ~~The frequency distribution of daily maximum MLH is shown in Fig. 2.~~ In this study, March, April and May are defined as spring; June, July and August are defined as summer; September, October and November are defined as autumn; and December, January and February are defined as winter.

To study the regional distribution characteristic of MLH on the NCP, we analyzed of the frequency of the daily maximum MLH distribution in Fig. 2. The daily maximum MLH at the BJ, SJZ and TJ stations ~~reached~~ could reach 2400 m.~~,~~ T~~and t~~he ~~high~~ large daily maximum values mostly ~~occurred~~ existed in spring and summer, while the low values always appeared~~occurred~~ in autumn and winter and were as low as 200 m. The daily maximum MLH values at the BJ, SJZ and TJ stations were mainly distributed between 600 and 1800 m, 400 and 1600 m and 800 and 1800 m, ~~respectively, and they~~ account~~inged~~ for 74.2, 72.0 and 67.0 % of the total samples, respectively. Notably, the daily maximum MLH ~~at~~ in SJZ was lower than ~~in spring, autumn and winter in comparison with those~~ the MLHs at the BJ and TJ stations in spring, autumn and winter. Values below 600 m at the SJZ station occurred primarily in autumn and winter~~; t~~. The most frequent daily maximum MLH ~~was~~ existed in the range of ~~from~~ 1000~~-~~ ~~to~~ 1200 m, which was 200-600 m lower than that at the TJ station. This ~~pattern~~ demonstrated a weaker atmospheric diffusion capability at the SJZ

带格式的: 字体: (国际) Times New Roman
带格式的: 字体: Times New Roman
带格式的: 字体: (国际) Times New Roman
带格式的: 字体: (国际) Times New Roman
带格式的: 字体: (国际) Times New Roman
带格式的: 字体: Times New Roman
带格式的: 字体: (国际) Times New Roman
带格式的: 字体: (国际) Times New Roman
带格式的: 缩进: 首行缩进: 0 厘米
带格式的: 字体: 小三, (国际) Times New Roman
带格式的: 字体: Times New Roman, 小三
带格式的: 字体: Times New Roman, 小三
带格式的: 字体: Times New Roman, 小三
带格式的: 字体: Times New Roman, 小三
带格式的: 字体: 小三, (国际) Times New Roman
带格式的: 字体: 小三, (国际) Times New Roman
带格式的: 字体: 小三, (国际) Times New Roman
带格式的: 字体: Times New Roman, 小三
带格式的: 字体: 小三, (国际) Times New Roman
带格式的: 字体: Times New Roman, 小三
带格式的: 字体: 小三, (国际) Times New Roman
带格式的: 字体: 小三, (国际) Times New Roman
带格式的: 字体: 小三, (国际) Times New Roman
带格式的: 字体: Times New Roman, 小三
带格式的: 字体: 小三, (国际) Times New Roman
带格式的: 字体: Times New Roman, 小三
带格式的: 字体: 小三, (国际) Times New Roman
带格式的: 字体: 小三, (国际) Times New Roman
带格式的: 字体: 小三, (国际) Times New Roman
带格式的: 字体: 小三, (国际) Times New Roman
带格式的: 字体: 非加粗

station in spring, autumn and winter than ~~th at~~ the northern NCP stations.

The frequency distribution of the daily maximum MLH at the coastal ~~station~~ site ~~was~~ showed different features. The daily maximum MLH ~~at~~ in QHD was mainly distributed between 800 and 1800 m with a relatively ~~uniform~~ small seasonal ~~distributions~~ fluctuation (Fig. 2d). Values lower than 600 m were mainly ~~occurred~~ distributed in summer, which was probably influenced by the frequent occurrence of a thermal internal boundary layer (TIBL) in summer. ~~(van der Kamp and McKendry, 2010).~~ Reasons for this are illustrated in section 4.1.

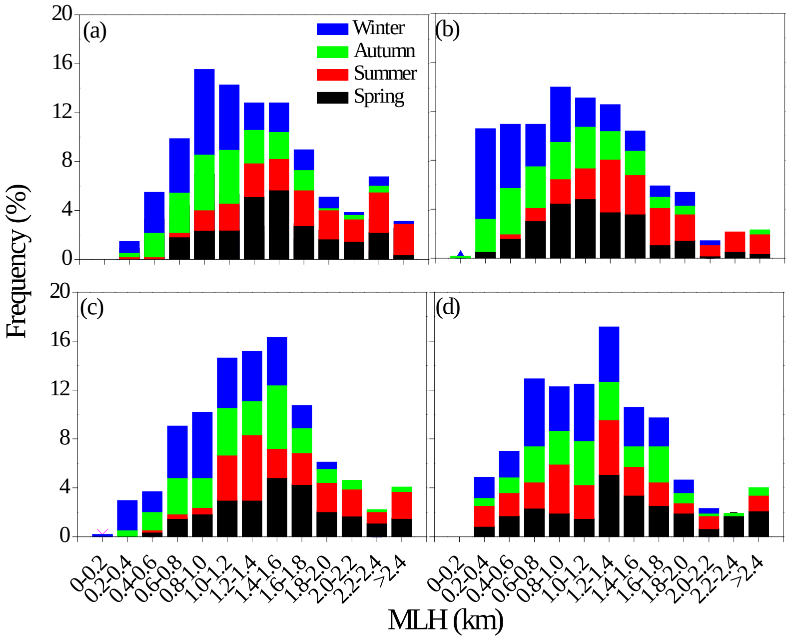

Fig. 2. Frequency distribution of the daily maximum MLH at the (a) BJ, (b) SJZ, (c) TJ and (d) QHD stations from December 2013 to November 2014.

3.2 Spatiotemporal variation of ~~regional~~ MLH

3.2.1 Seasonal variation

Monthly variations of MLH at the BJ, SJZ, TJ and QHD stations are shown in Fig. 3. The monthly means of the regional MLH ranged between 300 and 750 m. T~~; t~~he maximum and minimum MLH ~~occurred~~ existed in June 2014 at the BJ station and in January 2014 at the SJZ station, with values of 741 and 308 m, respectively. Most of the monthly averages were between 400 and 700 m, which accounted for 81.3 % of the total samples.

The MLH at the BJ, SJZ and TJ stations showed obvious seasonal variations with high values in spring and summer and low values in autumn and winter. Seasonal means of MLH at the three stations followed the same order: summer>spring>autumn>winter, with maximum values of 722±169, 623~~-~~±161 and 655±165 m in summer, respectively, and minimum values of 493±131, 347±153 and 436±178 m in winter, respectively (Table S2~~1~~). Obvious annual changes of the MLH with large ~~amplitude~~ values in spring and summer and low values in autumn and winter at the BJ, SJZ and TJ stations implied that MLH is influenced by seasonal changes of solar radiation~~, and in summer, the intense solar radiation favors the development of MLH~~ (Stull, 1988).

Nevertheless, the seasonal variation of MLH at the coastal site of Bohai was different from that at the inland stations. The MLH ~~at~~ in QHD exhibited a decreasing trend from spring to summer and an increasing trend from autumn to winter, ~~and~~ with the maximum seasonal mean ~~at QHD was~~ of 498±217 m in spring and the minimum seasonal mean ~~was~~ of 447±153 m in summer. Moreover, the MLH in spring and summer at QHD was much lower than those at other stations. Similar to our analysis of frequency distributions of daily maximum MLH in s~~S~~ection 3.1, the lower MLH at QHD in spring and summer mainly resulted from the frequent occurrence of the TIBL~~sea breeze (Fig. 5)~~. A detailed explanation of the TIBL impact was included in section 4.1. ~~This~~ The effect of ~~sea breeze~~TIBL on the coastal boundary layer was consistent with previous studies (Zhang et al., 2013; Tu et al., 2012), which demonstrated that ceilometers can properly retrieve the coastal MLH as well.

带格式的：缩进：首行缩进： 1 字符

带格式的：字体颜色：自动设置

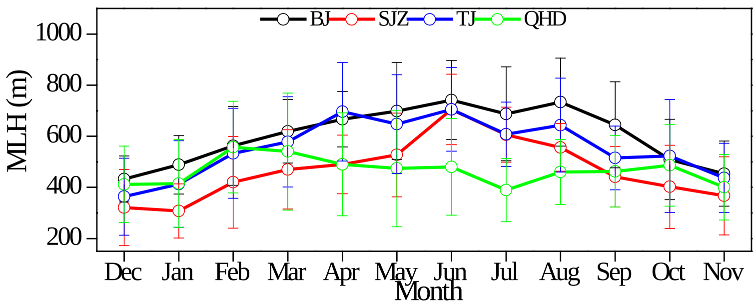

Fig. 3 Monthly variations of MLH at the BJ, SJZ, TJ and QHD stations from December 2013 to November 2014.

~~Annual averages of MLH at the BJ, SJZ, TJ and QHD stations were also calculated, and the values were 594±183, 464±183, 546±197 and 465±175 m, respectively. The MLH at SJZ was approximately 21.9, 15.0 and 0.2 % lower than at the BJ, TJ and QHD stations, respectively, which revealed a more stable atmospheric stratification and weaker atmospheric environment capability in southern Hebei.~~

3.2.2 Diurnal variations

Seasonal variations of diurnal MLH change patterns were investigated to reveal the 24 h evolution characteristics of the ~~regional~~ MLH on the NCP. As shown in Fig. 4, diurnal variations of ~~regional~~ MLH in different seasons all had single peak patterns. With sunrise and increased solar radiation, MLH at the four stations started to develop and peaked in the early afternoon. After sunset, turbulence in the MLH decayed quickly, and the mixing layer underwent a transition to the nocturnal stable layer (less than 400 m). The ~~averaged~~ annual averaged ~~daily~~ diurnal ranges of MLH at the BJ, SJZ, TJ and QHD stations were 782, 699, 914 and 790 m, respectively.~~, and t~~ The ~~averaged~~ annual averaged diurnal~~daily~~ range of MLH in~~at~~ SJZ was approximately 100-200 m smaller than those at the other stations, which was ~~. When we referred to the diurnal variations of regional MLH in different seasons, we found that the lower~~

~~annual daily range at the SJZ station was~~ associated with its ~~lower values of~~shallow daytime MLHs in spring, autumn and winter (Figs. 4a, 4c and 4d). This also indicated the worse pollutant diffusion ability in SJZ.

~~Average g~~Growth rates ~~for~~ averaged over the four stations during each season were plotted with gray columns in Fig. 4. It ~~demonstrated~~ was obvious that the growth rates of the ~~regional~~ MLH varied by season. The MLH developed the earliest in summer (at approximately 7:00 LT) and reached the highest growth rates (164.5 m h^{-1}) at approximately 11:00 LT, and the time when MLH started to develop was found to be 1 hour later (at approximately 8:00 LT) in spring and autumn than in summer. Furthermore, the MLH developed the latest (at approximately 9:00 LT) and slowest in winter, with the maximum growth rate (101.8 m h^{-1}) occurring at approximately 11:00 LT.

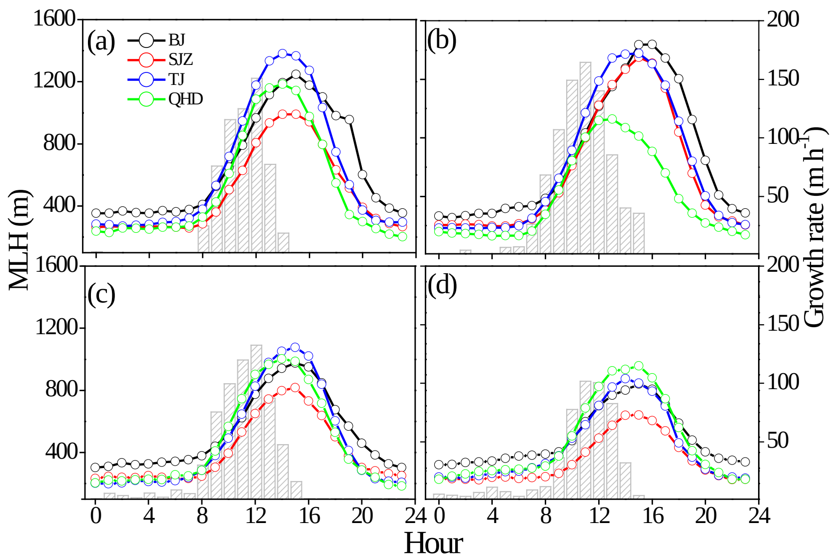

Fig. 4~~.~~ Diurnal variations of MLH at the BJ, SJZ, TJ and QHD stations in (a) spring, (b) summer, (c) autumn and (d) winter seasons are indicated by lines and scatters. The ~~averaged~~ growth rates averaged over~~at~~ the four sites are ~~depicted~~ drawn with gray columns for each season to represent the ~~regional~~ MLH growth velocity, and only positive values are shown in the figure.

~~Considering the MLH peak time and values, we also found that the Comparison of the MLH peaking time between the four stations showed that the maximum MLH at the TJ and QHD stations arrived earlier than those at the BJ and SJZ stations in spring and summer (Figs. 4a and 4b). However, in autumn and winter, such characteristic was not evident (Figs.4c and 4d).~~

~~When we came to the seasonal wind vectors distribution in the NCP region, we found that the sea breeze usually started at midday (approximately 11:00 LT) and prevailed during daytime at the QHD station in spring and summer (Fi).~~

~~As shown in Fig. 5, under the influence of the Siberian High and the geographic location effect, northerly and northwesterly winds prevailed in autumn and winter at~~

带格式的：缩进：首行缩进： 1 字符

带格式的：首行缩进： 0 字符

the four stations. In spring and summer, the northward lift and westward intrusion of a subtropical high causes the weak southerly wind to arrive and dominate in the NCP region. Without a large- or medium-scale weather system passing through, the sea breeze will play a role in the coastal area. Although the TJ station was supposed to be an inland site, it was still affected by the sea breeze to some extent. Due to the shoreline orientation and regional topography differences between TJ and QHD (Fig. 1), when a sea breeze occurred, easterly wind prevailed at the former station and easterly, and south-southwesterly wind blew at the latter station in spring and summer (Figs.5c and 5d). Statistical results revealed that from March 2014 to August 2014, the frequency of sea breeze occurrence at the TJ and QHD stations could reach 53.8 and 92.4 %, respectively, and the sea breeze usually started at midday (approximately 11:00 LT).

Generally, the vertical development of the mixing layer is heavily reliant on the vertical turbulence, but when sea breeze is present, cool air advection from the sea breeze circulation will suppress this vertical mixing intensity (Puygrenier et al., 2005). The co-existence of vertical turbulence and advection caused the MLH to decrease and peak earlier. Meanwhile, the local mixing layer will be replaced by the thermal internal boundary layer (Tomasi et al., 2011). As a result, the earlier peaking time of MLH in spring and summer could be attributed to the sea breeze effect. The MLH peaking time at the TJ station was approximately 1-2 hours later than at the QHD station, which indicated that such a sea breeze impact will weaken with distance from the coast (Huang et al., 2016).

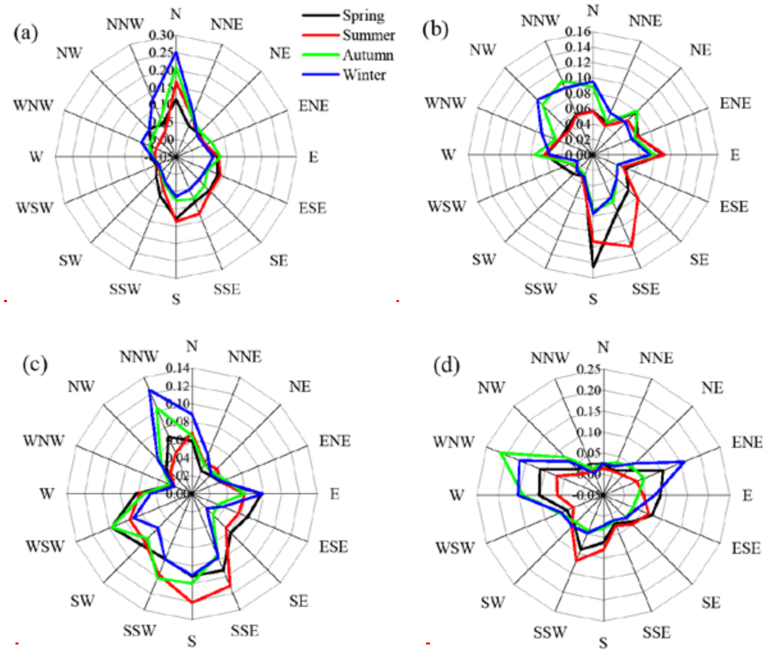

带格式的

带格式的: 左，定义网格后不调整右缩进，不调整西文与中文之间的空格，不调整中文和数字之间的空格

~~Fig. 5 Frequency of wind direction at the (a) BJ, (b) SJZ, (c) TJ and (d) QHD stations in different seasons.~~

Annual averages of MLH at the BJ, SJZ, TJ and QHD stations were also calculated, and the values were 594±183, 464±183, 546±197 and 465±175 m, respectively. The MLH at SJZ was approximately 21.9, 15.0 and 0.2 % lower than at the BJ, TJ and QHD stations, respectively. Therefore, according to the analysis above in sections 3.1 and 3.2, an obvious phenomenon can be observed in the MLH distribution on the NCP: the MLH in southern Hebei was lower than in the northern NCP in spring, autumn and winter but was almost equal to the northern areas in summer.~~Annual averages of MLH at the BJ, SJZ, TJ and QHD stations were also calculated, and the values were 594±183, 464±183, 546±197 and 465±175 m, respectively. The MLH at SJZ was approximately 21.9, 15.0 and 0.2 % lower than at the BJ, TJ and QHD stations, respectively, which revealed a more stable atmospheric stratification and weaker atmospheric environment capability in southern Hebei. ThereforeIn all, according to the analysis above in Sections 3.1 to 3.2, an obvious phenomenon can be observed in the MLH distribution in the NCP region: the MLH was lower in southern Hebei than on the northern NCP in spring, autumn and winter but was almost equal to the northern areas in summer.~~

4. Discussion

~~4.~~ Through preliminary study of the spatiotemporal variation of MLH on the NCP region, we found something interesting: (a) the MLH at the coastal site was lower than the inland sites in summer; (b) the MLH in southern Hebei was lower than the northern NCP in spring, autumn and winter, but was almost consistent between these two areas in summer. Reasons for these two phenomena will be illustrated in the following sections (4.1 and 4.2). Finally, we will investigate the meteorological evidence for serious haze pollution in southern Hebei in section 4.3.

4.1 ~~Reasons for low MLH in southern Hebei~~The TIBL impact in coastal site

From the studies in sections 3.1 and 3.2, we found that the maximum MLH at the QHD station was larger and arrived earlier than the BJ, SJZ and TJ stations in summer (Fig. 4b). However, this characteristic was not evident in other seasons (Figs. 4a, 4c and 4d). The sea-land breeze was a local circulation that occurs when there is no large-scale synoptic system passes. In our study, we first excluded days with large-scale synoptic systems. Then, according to the coastline orientation, if the southeast wind at the TJ station and south and southwest winds at the QHD station occurred at approximately 11:00 LT, and the northwest wind started to blow at approximately 20:00 LT, then this type of circulation was supposed to be a sea-land circulation. The prevailing southeast wind at the TJ station and the south and southwest wind at the QHD station were regarded as sea breezes (Fig. 5).

The sea breeze usually brings a cold and stable air mass from the sea to the coastal region. When the top of the local mixing layer was higher than the top of the air mass, a TIBL will develop within the mixing layer under the influence of the abrupt change of aerodynamic roughness and temperature between the land and sea surfaces. Then, the local mixing layer will be replaced by the TIBL. In the presence of warm air on land, the cold sea air advects downwind and is warmed, leading to a

带格式的: 缩进: 首行缩进: 1 字符

带格式的: 正文, 无项目符号或编号

带格式的: 字体: (默认) Times New Roman, 小四, 加粗

带格式的: 正文, 无项目符号或编号

带格式的: 字体: (默认) Times New Roman, 小四

带格式的: 字体: (默认) Times New Roman, 小四

带格式的: 字体: (默认) Times New Roman, 小四

带格式的: 字体: (默认) Times New Roman, 小四

带格式的: 字体: (默认) Times New Roman, 小四

带格式的: 字体: (默认) Times New Roman, 小四

带格式的: 字体: (默认) Times New Roman, 小四

带格式的: 字体: (默认) Times New Roman, 小四

带格式的: 字体: (默认) Times New Roman, 小四

带格式的: 字体: (默认) Times New Roman, 小四

带格式的: 字体: (默认) Times New Roman, 小四

带格式的: 字体: (默认) Times New Roman, 小四

带格式的: 字体: (默认) Times New Roman, 小四

带格式的: 字体: (默认) Times New Roman, 小四

带格式的: 字体: (默认) Times New Roman, 小四

带格式的: 字体: (默认) Times New Roman, 小四

带格式的: 字体: (默认) Times New Roman, 小四

weak temperature difference between the air and the ground. In consequence, the TIBL warms less rapidly due to the decreased heat flux at the ground, and the rise rate is reduced. In addition, since the TIBL deepens with distance downwind and usually can not extend all the way to the top of the intruding marine air, the remaining cool marine air above the TIBL will hinder vertical development of the TIBL (Stull, 1988; Sicard et al., 2006; Puygrenier et al., 2005; Tomasi et al., 2011). With distance inland, the top of the intruding marine air will enhance and exceed the local MLH; if so, the TIBL will not form, and the TIBL impact will be impaired with distance inland (Stull, 1988). Accompanied by the weak synoptic system and the frequent occurrence of sea breezes in summer, the TIBL formed easily and the MLH peak time and value at the QHD station were earlier and lower than other stations (Figs. 3 and 4). For the TJ station, with a distance of approximately 50 km out to sea, the TIBL will not extend so far. Therefore, although the TJ station can be affected by the sea breeze, the local MLH cannot be influenced by the TIBL.

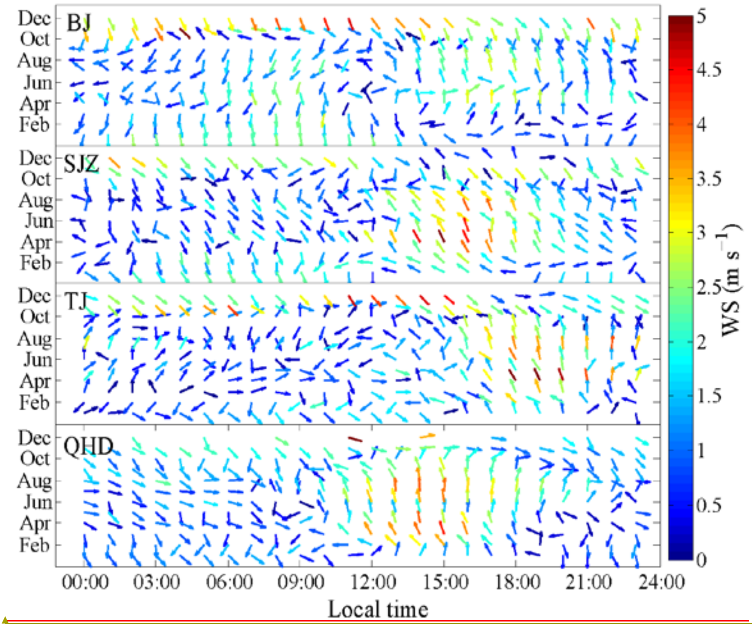

Fig. 5 Monthly diurnal wind vectors at the BJ, SJZ, TJ and QHD stations from December 2013 to November 2014.

~~4.1~~4.2 Reasons for low MLH in southern Hebei

Turbulent ~~energy~~ stability was mainly responsible for the MLH development, and the generation of turbulent energy was highly correlated with the ~~buoyancy~~ heat flux (mainly sensible heat ~~and moisture~~ fluxes) produced by ~~net~~ radiation and the momentum flux caused by wind shear (Stull, 1988). As presented in section 2.4, the *Ri* could describe the turbulent stability not only from the perspective of thermal forces but also from the perspective of mechanical forces; it was calculated in this section with meteorological sounding profiles to study the reason for MLH differences between southern Hebei and the northern NCP, and the frequency values

带格式的: 字体: (默认) Times New Roman, 小四
带格式的: 字体: (默认) Times New Roman, 小四
带格式的: 字体: (默认) Times New Roman, 小四
带格式的: 字体: (默认) Times New Roman, 小四
带格式的: 字体: (默认) Times New Roman, 小四
带格式的: 字体: (默认) Times New Roman, 小四
带格式的: 字体: (默认) Times New Roman, 小四
带格式的: 字体: (默认) Times New Roman, 小四
带格式的: 字体: (默认) Times New Roman, 小四
带格式的: 字体: (默认) Times New Roman, 小四
带格式的: 字体: (默认) Times New Roman, 小四
带格式的: 字体: (默认) Times New Roman, 小四
带格式的: 字体: (默认) Times New Roman, 小四
带格式的: 正文, 居中, 无项目符号或编号
带格式的: 字体: (默认) Times New Roman, 小四
带格式的: 正文, 无项目符号或编号
带格式的: 字体: (默认) Times New Roman, 小四
带格式的: 字体: 非倾斜
带格式的: 字体: 倾斜

of *Ri*>1 were given in this study. With larger frequency comes more stable stratification. Considering the geographic locations (Fig. 1), the lack of sounding data at the SJZ station was replaced by sounding data from the XT station; meanwhile, sounding data from the LT station was used instead of the data from QHD. Each of the four parameter profiles (WS, shear term, buoyancy term, and the frequency of *Ri*>1) at the BJ, XT and LT stations are depicted in Fig. 6. The profiles were averaged over 8:00 LT and 20:00 LT and vertically smoothed using a 100-m running average to reduce unexpected fluctuations for viewing purposes only. We first compared the net radiation among the BJ, SJZ and TJ observation sites. As shown in Fig. 6, the seasonal net radiation variations were almost consistent among the three stations, and they were high in spring and summer and low in autumn and winter, with annual averages of 5.4, 6.0 and 4.8 W m^{-2}, respectively. The comparable net radiation values at the BJ and SJZ stations indicated that the buoyancy flux was unable to explain the MLH differences between the northern NCP and southern Hebei.

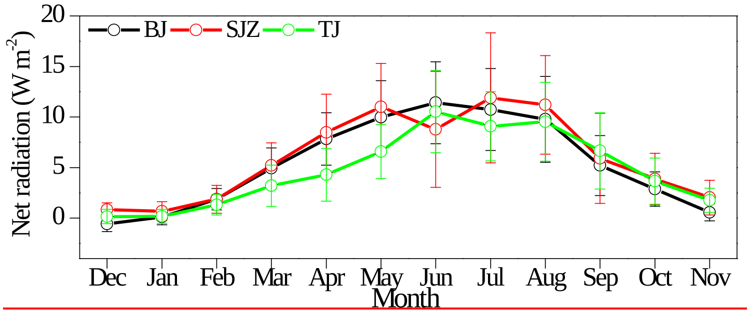

Fig. 6 Monthly variations in net radiation at the BJ, SJZ and TJ sites.

Wind shear was defined and calculated according to Eq. (1):

wind shear =(1)

where is the height difference between two layers at which the vertical wind shear is estimated and are the differences in zonal and meridional directions in the two different layers (Hyun et al., 2005). Considering the geographic locations (Fig. 1), the lack of sounding data at the SJZ station was addressed by replacement with sounding data from another southern Hebei station (e.g., the XT station); meanwhile, sounding data from another coastal site (e.g., the LT station) were used instead of from the QHD station. Observations were conducted at 8:00 LT and 20:00 LT each day from December 2013 to November 2014, and the wind shear was averaged every 100 m for each sounding profile.

带格式的：字体：倾斜

带格式的：两端对齐，缩进：首行缩进： 1 字符

带格式的：两端对齐，缩进：首行缩进： 1 字符

带格式的：缩进：首行缩进： 1 字符

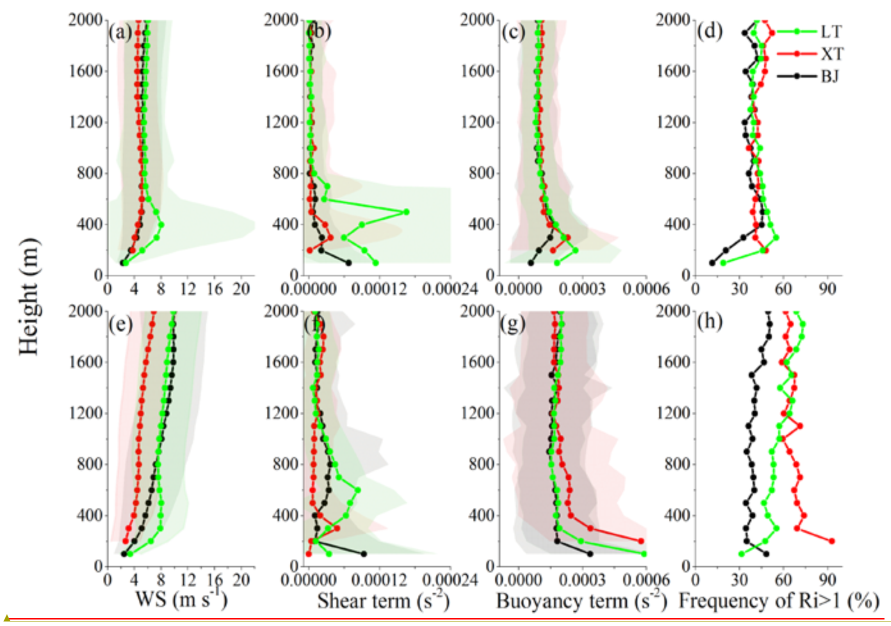

Fig. 6 Vertical profiles of (a, e) horizontal WS, (b, f) shear term, (c, g) buoyancy term and (d, h) frequency of *Ri*>1 at the BJ, XT and LT stations in summer (upper panel) and winter (lower panel).

TookUsing the winter and summer as examples, When when we analyzed the seasonal means of wind shear terms and the buoyancy term –between the southern Hebei (XT) and the northern NCP (BJ) stations, some distinct features were observed., As shown in Figs. 6f and 6g,. cConsidering that the regional MLH at 08:00 LT and 20:00 LT was mostly below 300 m in winter (Fig. 4), the wind shear terms and the buoyancy term in southern Hebei XTwere was 2.8 times lower and 1.5 times higher than those that in the northern NCPBJ within 0-1200 m in winter, respectively. below 300 m but were nearly consistent at the altitude of 300 m both at 08:00 LT and 20:00 LT during the whole year. However, above 300 m at 08:00 LT, wind shears at XT weresignificantly different from thoseat BJ again at the altitude of 300-1700 m and, on average, approximately 2.8, 2.5 and 1.9 times smaller than that at thein BJ stations in spring, autumn and winter, respectively (Figs. 7a, 7c and 7d)., and tThe largest discrepancies of the wind shear term and buoyancy term between southern Hebei and the northern NCP could reach 2.84×10^{-5} s^{-2}ed 3.4, 4.3, and 4.5 m s^{-1} km^{-1} in spring, autumn and winter, respectively, and were at the altitude of between500 and 7800 m and 3.93×10^{-4} s^{-2} at 200 m, respectively. As a result, the frequency of *Ri*>1 in XT was approximately 3.71.9 times larger than that in BJ within 0-1200 m, leading to a much more stable stratification in southern Hebei (Fig. 6h). The shear term, buoyancy term and the frequency of *Ri*>1 in spring and autumn displayed similar characteristics to those in winter, and the averaged frequency of *Ri*>1 in southern Hebei was approximately 1.5 and 1.3 times larger than those in northern NCP in spring and autumn, respectively (Fig. S3). While iIn summer, the averaged differences

带格式的：字体：(默认) Times New Roman, 小四

带格式的：居中

带格式的：字体：倾斜

带格式的：字体：倾斜

~~narrowed down to only 1.2-foldwind shear~~shear term, buoyancy term and the frequency of *Ri*>1 were almost the same between southern Hebei and the northern NCP~~-above 300 m~~ (Figs. 6~~7~~b, 6c and 6d).~~ Compared to wind shears at 20:00 LT above 300 m in spring, autumn and winter, mechanical forces were clearly enhanced in BJ at the height of 300-1700 m during the whole night and the turbulent energy was restored in the residual layer. With the increase of solar radiation in the morning, the MLH developed and broke through the residual layer. At this time, the combination of buoyancy and wind shear forces will contribute to a higher MLH at BJ during daytime. Furthermore, the larger wind shears below 300 m during night time at the BJ station could partly explain the higher nocturnal boundary layer on the northern NCP (Fig. 4).~~

带格式的: 字体: 倾斜

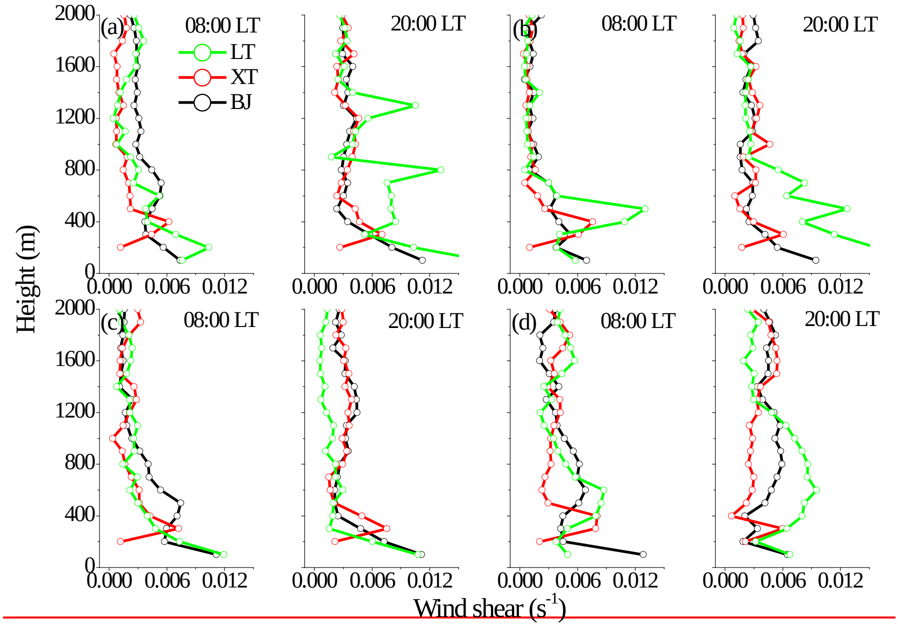

~~Fig.7 Vertical profiles of wind shear at the BJ, XT and LT stations in (a) spring, (b) summer, (c) autumn and (d) winter.~~

As a result, t~~T~~he lower MLH in southern Hebei was ~~the result of~~ due to a ~~the~~ more stable atmospheric turbulent structure than the northern NCP ~~lessened mechanical forcing due to wind shear at night than occurred in the northern areas~~ in spring, autumn and winter. This probably resulted from the frequent effect of cold air on the northern NCP, and such cold air was usually too weak to reach southern Hebei (Su et al., 2004). Then the cold front resulting from the cold air system will enhance the wind shear over the northern NCP. In addition, a previous study has revealed that the warm advection from the Loess Plateau usually developed from south to north, and the lower MLH in southern Hebei will be partially related to the enhance thermal inversion at the altitude of 1500 m (Hu et al., 2014; Zhu et al., 2016). In summer, due to the northward lift and westward intrusion of the subtropical high on the NCP, the diminishing existence of the weak cold air on the northern NCP accompanied with the regional scale strong solar radiation and strong turbulent activities will lead to a small turbulent stability contrast between southern Hebei and the northern NCP.This pattern could be attributed to the influence of the active fronts passing by under the impact of the Siberian High, and usually, this front system does not reach southern Hebei. In summer, due to the influence of the subtropical high on the NCP and the relatively greater solar radiation, the lessened effects of the front system and strong turbulent exchange will lead to less wind shear contrast in the vertical direction between southern Hebei and the northern NCP.

In addition, other researchers proposed that absorbing aerosols above the MLH can be another factor affecting the MLH (Peng et al., 2016; Wang et al., 2013; Li et al., 2016). Absorbing aerosols gives rise to an increasing temperature aloft but a decreasing temperature at the surface, which will enhance the strength of capping inversion and inhibit the convective ability. In contrast, absorbing aerosols within the mixing layer could reduce the capping inversion intensity despite the reduction in the surface buoyancy flux and raise the MLH (Yu et al., 2002). Considering the higher concentrations of surface $PM_{2.5}$ in southern Hebei, absorbing aerosols could have some impacts on MLH development. However, the comprehensive influences from the feedback of absorbing aerosols above and below the MLH are hard to explain without sufficient knowledge of vertical variations in absorbing aerosols at the four stations. Additionally, the mixed state and morphology of absorbing aerosols dominant the absorption effects (Jacobson, 2001; Bond et al., 2013). Therefore, without sufficient observation data, it is difficult to discuss the possible influences of air pollution feedback on MLH development in this study. Elaborate experiments of vertical profiles and the morphology of absorbing aerosols are needed in future studies.

4.24.3 Meteorological evidence of serious air pollution in southern Hebei

When we analyzed the near-ground $PM_{2.5}$ and PM_{10} concentrations distributions on the NCP from December 2013 to November 2014, a unique phenomenon was found and shown in Fig. 1 and Fig. S43. The annual means of near-ground $PM_{2.5}$ concentration in southern Hebei (SJZ, XT, HS, and HD and DZ) was 133.3 124.1μg m^{-3} (218.8225.3 μg m^{-3} for the PM_{10} concentrations), while in the northern areas (BJ, TJ, LF and TJS), it was 86.594.9 μg m^{-3} (145.5126.0 μg m^{-3} for the PM_{10} concentrations), and the difference in the near-ground $PM_{2.5}$ concentration between thesese two areas can be as high as 1.553-fold (1.51.8-fold for the PM_{10} concentrations). Since AOD represents the aerosol column concentration, it is a much better indicator for the emissions difference than the $PM_{2.5}$. Additionally, the averaged annual AOD in southern Hebei was only 1.2 times of that in the northern NCP (Fig. 7). If the difference in AOD represents the emission discrepancy, the remaining differences of $PM_{2.5}$ may be induced by the meteorology. In other words, meteorological conditions may play an important role in pollutants contrast between heavier haze formation in southern Hebei and the meteorological condition contrast between these two areas contributed approximately 60% to the $PM_{2.5}$ concentration discrepancy. Considering the lower MLH in southern Hebei, the heaviery pollution in southern Hebei may be related with weaker weather conditions, and some other meteorological factors may play a part.

带格式的：缩进：首行缩进： 1 字符，定义网格后不调整右缩进，不调整西文与中文之间的空格，不调整中文和数字之间的空格

带格式的

带格式的：缩进：首行缩进： 1 字符

带格式的：下标

带格式的：下标

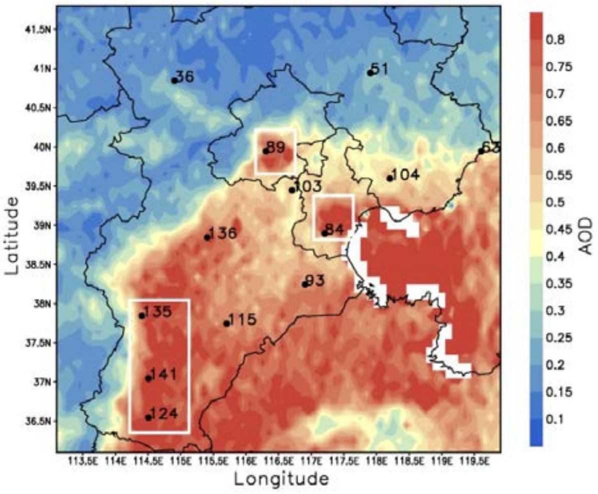

Fig.7 Distribution of the annual mean values of AOD from December 2013 to November 2014 in the NCP. The $PM_{2.5}$ concentrations of the 13 observation sites were also marked beside each station. The major sites in the northern NCP (BJ and TJ) and southern Hebei (SJZ, XT and HD) are enclosed by white rectangles.

Previous studies revealed that the most significant meteorological factors for regional heavy haze formation i~~o~~n the NCP were RH and MLH (Tang et al., 2016; Zhu et al., 2016). In addition, the T influences the particles' physicochemical reaction rate and the ventilation coefficients (V_c) can be used as an index to evaluate the total diffusion ability of the atmosphere; thus, the RH, T and V_c were compared and analyzed among the four stations (BJ, SJZ, TJ and QHD) in the next section. The regional particle growth and the atmospheric dissipation ability will be discussed separately, each from a meteorological point of view. ~~However, due to the lack of wind profiles, Tang et al. (2015) utilized the near-surface WS to estimate the ventilation coefficients (V_c), and the result was not sufficiently precise and could not portray the regional pollution dissipation ability accurately. In this study, we utilized wind sounding data to enable an exact evaluation of the regional pollutant dissipation ability. Furthermore, temperature is the main factor in new particle formation, and RH determines the growth rates of particles, which are the most influential meteorological factors for particle formation. As a consequence, in the next section, we will separately analyze the regional particle formation and dissipation ability, each from a meteorological point of view.~~

4.~~2~~3.1 Meteorological factors for particle ~~formation and~~ growth

~~Monthly variations~~Distributions of annual means of T and RH are shown in Fig. 8, and the distributions of seasonal means of T and RH were added in Figs. S5 and ~~Fig.~~ S6~~-~~. The T value in ~~the~~ southern Hebei was similar to that on the northern NCP ~~— in variation pattern and quantity~~ but was ~~approximately 19.3 %~~ higher than that at the coastal site (Figs. 8a and S5). This indicated an almost consistent temperature condition for an atmospheric physicochemical reaction (Garratt et al., 1994~~Tang et al., 2006~~; Zhang et al., 2010). ~~Under the same temperature conditions, the new particle~~

带格式的: 字体: (默认) Times New Roman, 小四

带格式的: 字体颜色: 红色

带格式的: 字体: 非加粗

~~formation ability will be the same between these two areas.~~ However, differences existed in RH between southern Hebei and the northern NCP. The RH ~~at~~ in the SJZ station was always higher than that ~~at~~ in the BJ and TJ stations but was slightly lower than that at the coastal sites ~~at the QHD station through the year~~ (Figs. 8b and S6). The annual averages of RH at the BJ, SJZ, TJ and QHD sites were 51.2, 65.7, 57.0 and 68.6 %, respectively, and the RH at SJZ was 22.1 and 13.2 % higher than that at the BJ and TJ sites, respectively (Table S3~~2~~). Since~~As~~ RH is ~~also~~ a key factor for haze development, higher RH is beneficial to fine particle growth through hygroscopic growth processes and heterogeneous reactions (Zhao et al., 2013; Fu et al., 2014; Liu et al., 2011; Hu et al., 2006; Zhang et al., 2015; Seinfeld et al., 1998). ~~and determines the particle growth rate through hygroscopic growth and secondary formations (Zhao et al., 2013; Fu et al., 2014), even though the new particle formation conditions were the same between these two areas, particles can grow larger under high RH,~~ Thus, a higher RH provided a favorable meteorological condition for haze development, which could be partially responsible for heavier pollution in southern Hebei.~~leading to heavier pollution in southern Hebei.~~

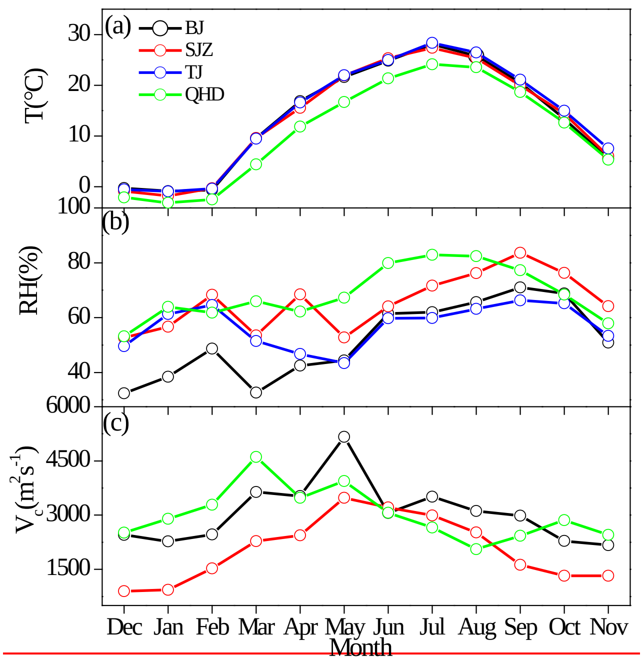

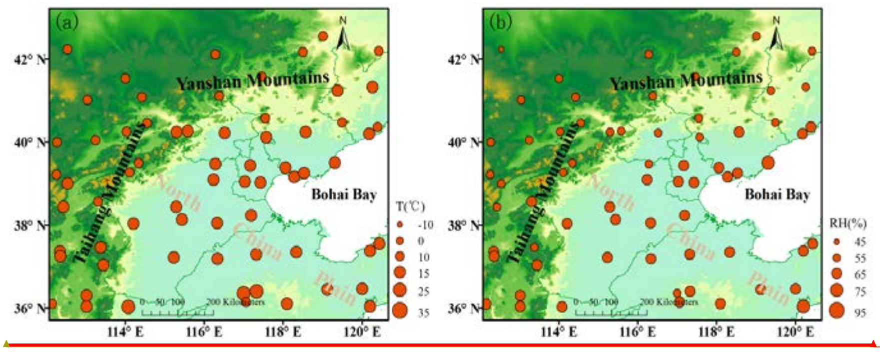

Fig. 8 Distribution of annual means of (a) T and (b) RH in the NCP region from December 2013 to November 2014.

~~Fig. 8 Seasonal variations of (a) T, (b) RH and (c) V_c at the BJ, SJZ, TJ and QHD stations from December 2013 to November 2014. The V_c is defined as the product of MLH to the wind transport (Nair et al., 2007) (Eq. (2)). With larger V_c, strong dissipation ability follows.~~

4.~~2~~3.2 Meteorological factors for particle dissipation

As MLH and WS can represent the atmospheric dissipation capability in the vertical and horizontal directions, respectively, in addition to the MLH, we ~~also~~ analyzed the WS variations on the NCP. Similar to our analysis in s~~S~~ection 4.2~~1~~, as SJZ and QHD had no sounding data and due to the close geographic proximity among SJZ and XT as well as LT and QHD, sounding data from the XT and LT stations were used instead of the data at SJZ and QHD, respectively. The WS profiles were averaged every 100 m at each station~~s~~ and are depicted in Figs. ~~S2~~6 and S3. Except for summer, the WS in southern Hebei was far less than that on the northern NCP ~~and coastal areas both at 08:00 LT and 20:00 LT~~ in spring, autumn and winter (Figs. 6e, S3~~2~~a~~,~~ ~~S2c~~ and S3e ~~and S2d~~) but was nearly consistent in summer (Fig. ~~S2b~~6a). This finding indicated a weaker horizontal diffusion capability in southern Hebei than that on the northern NCP ~~and at the coastal sites~~.

The V_c ~~ventilation coefficient~~ is an important factor in pollutant dissipation and air quality studies; it accounts for the vertical dispersion and advection of pollutants. With a larger V_c, strong dissipation ability follows. The V_c is defined as the product of MLH ~~to the~~and wind transport (U_T) ~~and is~~as shown in Eq. (2).

$$V_c = MLH \times U_T \quad (2)$$

When we utilized the wind profiles in Figs. 6 and S3~~S2~~ with equal spacing in the vertical direction, U_T could be regarded as the mean wind transport, i.e., $U_T = \frac{1}{n}\sum_{i=1}^{n} U_i$ ~~U_T=~~, ~~and~~ where U_i is the ~~wind~~ WS observed at each level and n is the number of levels within the mixing layer (Nair et al., 2007). Since the WS was a climatic parameter, the WS profiles at 08:00 LT and 20:00 LT were used to approximate V_c approximately. ~~As the profiles of WS for each station were almost the same in the morning and at night (Fig. S2), it was considered reasonable to regard the sounding data of WS as a climatological constant, and the V_c within the mixing layer~~

带格式的：字体：(默认) Times New Roman，小四，加粗，字体颜色：文字 1

带格式的：定义网格后不调整右缩进，不调整西文与中文之间的空格，不调整中文和数字之间的空格

带格式的：字体：加粗，字体颜色：文字 1

带格式的：两端对齐

带格式的：下标

~~could then be calculated.~~ Considering the monthly averaged MLH at the BJ, SJZ and QHD stations, the monthly V_c ~~is~~ were depicted in Fig. ~~8c~~9. V_c at ~~the~~ southern Hebei was always lower than that in the northern NCP during the whole study period. The seasonal means of V_c at the BJ, SJZ and QHD stations in spring, summer, autumn and winter were 4112.0, 2733.3 and 4008.5; 3227.5, 2908.8 and 2593.7; 2481.4, 1421.9 and 2581.7; and 2397.2, 1117.7 and 2900.0 $m^2\ s^{-1}$, respectively. It was clear that the SJZ station usually had the lowest V_c, and the annual averaged V_c at SJZ was almost 1.5 and 1.5 times smaller than the BJ and QHD stations, respectively (Table S3~~2~~). As a result, the particle dissipation capability in southern Hebei was much weaker than that in the northern NCP and coastal areas.

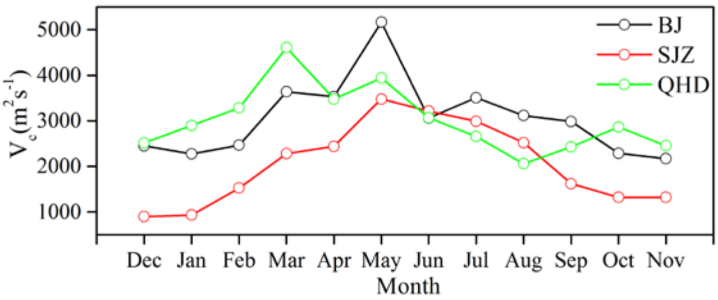

Fig. 9 Seasonal variations of V_c at the BJ, SJZ and QHD stations from December 2013 to November 2014. The V_c is defined as the product of MLH and wind transport (Nair et al., 2007) (Eq. (2)). With a larger V_c, strong dissipation ability follows.

Therefore, with~~due to the~~ lower ~~atmospheric environment capability~~MLH, lower WS and higher RH occur ~~, the weaker dissipation ability and stronger particle formation ability, the particles were more easily accumulated and severe haze occurred frequently~~ in southern Hebei compared to the northern NCP, the near-ground $PM_{2.5}$ showed a large contrast between these two areas. However, the AOD had little difference between southern Hebei and the northern NCP. Apart from the emission contrast, the meteorological condition contrast between these two areas heavily contributed to the –heavy haze in southern Hebei and~~that~~ the industrial structure ~~of southern Hebei~~ is in need of readjustment for the NCP (Fig. 10).

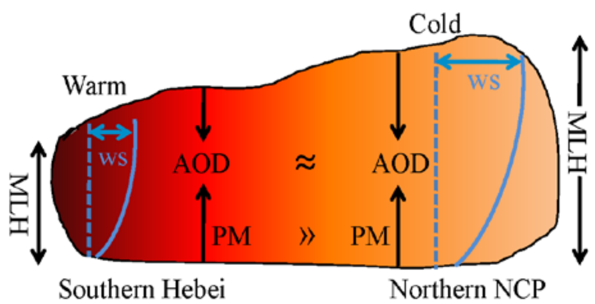

Fig.10 The schematic diagram of the meteorological causes for heavy haze in southern Hebei.

带格式的: 字体: (默认) Times New Roman, 小四

带格式的: 字体: (默认) Times New Roman, 小四

带格式的: 居中, 首行缩进: 0 字符

带格式的: 左, 缩进: 首行缩进: 0 字符

5. Conclusions

To gain new insight into the spatiotemporal variation of the regional MLH, the present study conducted a simultaneous observation with ceilometers at three inland stations (~~e.g.,~~ BJ, SJZ, and TJ) and one coastal site (~~e.g.,~~ QHD) to obtain high spatial and temporal resolution MLH data. The experiment period lasted for 22-months from October 16, 2013, to July 15, 2015, and ~~one~~ a whole year~~'s~~ of data (~~e.g.,~~ from December 2013 to November 2014) were utilized for further study. Conclusions were drawn as follows.

The ceilometers can not only retrieve the inland MLH but also retrieve the coastal MLH properly. The MLHs in the inland areas of the NCP ~~was~~ were high in spring and summer and low in autumn and winter. While under the impact of TIBL, the coastal MLH had an opposite variation trend of inland sites ~~Under the effects of sea breeze and a thermal internal boundary layer, the seasonal variation of the MLH in the coastal area of Bohai was different from that of the inland stations,~~ and the lowest MLH in QHD ~~was~~ occurred in summer. The TIBL impaired the local MLH development at the coastal site and caused the mixing layer to~~MLH~~ peak~~ed~~ ~~earlier~~ early ~~at the coastal site~~ in ~~spring and~~ summer ~~than at the inland stations~~; ~~and~~ this effect weakened with distance ~~from the coast~~inland. ~~This effect of sea breeze on coastal MLH was consistent with previous studies, which demonstrated that not only can the mainland MLH be retrieved from ceilometers, but the coastal MLH can be observed with ceilometers.~~

The MLH in southern Hebei was lower than that on the northern NCP, especially in spring, autumn and winter. This ~~As there was little radiation difference between these two areas, the lower MLH in the southern Hebei~~ mainly resulted from the more stable turbulent structure (weak shear term, higher buoyancy term and larger frequency of *Ri*>1) than ~~stronger intensity of wind shears on~~ the northern NCP~~.than in southern Hebei at an altitude of 300-1700 m in residual layers~~, and the stable stratification in southern Hebei was partially related to the Siberian High and warm advection from the Loess Plateau. ~~–~~ In summer, the~~–~~ atmospheric stability was almost consistent between southern Hebei and the northern NCP~~wind shear difference lessened~~, and the MLHs between th~~e southern and northern~~ese two areas were nearly identical~~consistent~~.

~~From a meteorological point of view, t~~The lower MLH and WS in southern Hebei restricted the atmospheric environmental capability and the pollutant dissipation ability, respectively. ~~weaker atmospheric environment capability~~ Accompanied by~~combined with the weaker~~ higher RH values ~~pollutant dissipation ability and the stronger pollutant formation ability~~(stronger pollutant growth ability), the adverse weather conditions will cause severe haze to occur easily in southern Hebei, and the industrial layout in ~~southern Hebei~~the NCP is in need of restructuring. Heavily polluting enterprises should be relocated to locations with better weather conditions (e.g., ~~certain~~ some northern areas and coastal areas), and strong emission reduction measures should be implemented in the remaining industrial enterprises to improve air quality.

Overall, the present study is the first to conduct a long-term observation of the

带格式的: 字体: 倾斜

MLH with high spatial and temporal resolution on a regional scale. The observation results will be of great importance for model parameterization scheme promotion and provide basic information for the distribution of weather conditions in the NCP region. The deficiency of this study is that we ~~took no~~did not account ~~of~~ for the transport effect on $PM_{2.5}$ concentrations. Because pollutants are usually transported from south to north in the NCP region during haze episodes (Zhu et al., 2016; Tang et al., 2015), ~~the~~ pollutant transport has a greater impact on the northern areas and ~~had~~ has less ~~of an~~ influence on the results of this analysis. The absence of sounding data at noon is another shortcoming, and ~~we plan to conduct~~ the daytime observations will be implemented in future experiments. Nevertheless, our study can provide reasonable and scientific suggestions for industrial layout and air pollution emission~~s~~ reduction measures for the NCP region, which will be of great importance for achieving the integrated development goals.

Acknowledgments

带格式的: 字体: 加粗

This work was supported by the National Key R&D Program of China (2017YFC0210000), the National Natural Science Foundation of China (41705113), the Beijing Municipal Science and Technology Project (ZL171100000617002)~~This work was supported by the CAS Strategic Priority Research Program (Grant no.XDB05020000), the National Natural Science Foundation of China (Grant no.41230642)~~ and the National Earth System Science Data Sharing Infrastructure, National Science & Technology Infrastructure of China.

References

Alexander, G., M. Wiegner, B. Bonn, K. Schäfer, R. Forkel, E. V. Schneidemesser, C. Münkel, K. L. Chan, and R. Nothard: Mixing layer height as an indicator for urban air quality? Atmos. Meas. Tech., 10, 2969-2988, doi.org/10.5194/amt-10-2969-2017, 2017.

Beyrich, F.: Mixing height estimation from SODAR data – a critical discussion, Atmos. Environ., 31, 3941–3953, 1997.

Bond, T. C., et al.: Bounding the role of black carbon in the climate system: a scientific assessment, J. Geophys. Res., 118, 1-173, doi:10.1002/jgrd.50171, 2013.

Chen, W., Kuze, H., Uchiyama, A., Suzuki, Y., and Takeuchi, N.: One-year observation of urban mixed layer characteristics at Tsukuba, Japan using a micro pulse lidar, Atmos. Environ., 35, 4273–4280, doi:10.1016/S1352-2310(01)00181-9, 2001.

Emeis, S., C. Münkel, S. Vogt, W. J. Müller, and K. Schäfer: Atmospheric boundary-layer structure from simultaneous SODAR, RASS, and ceilometer measurements, Atmos. Environ., 38(2), 273-286, doi:10.1016/j.atmosenv.2003.09.054, 2004.

Emeis, S., K. Schäfer, and C. Münkel: Observation of the structure of the urban boundary layer with different ceilometers and validation by RASS data, Meteorologische Zeitschrift, 18(2), 149-154, doi:10.1127/0941-2948/2009/0365, 2009.

Emeis, S., K. Schäfer, C. Münkel, R. Friedl, and P. Suppan: Evaluation of the Interpretation of Ceilometer Data with RASS and Radiosonde Data, Bound.-Lay. Meteorol., 143(1), 25-35, doi:10.1007/s10546-011-9604-6, 2011.

Eresmaa, N., Karppinen, A., Joffre, S. M., Räsänen, J., and Talvitie, H.: Mixing height determination by ceilometer, Atmos. Chem. Phys., 6, 1485–1493, doi: 10.5194/acp-6-1485-2006, 2006.

Fu, G., W. Xu, R. Yang, J. Li, and C. Zhao: The distribution and trends of fog and haze in the North China Plain over the past 30 years, Atmos. Chem. Phys., 14 (21), 11949-11958, 2014.

Garratt J., The atmospheric boundary layer. Cambridge University Press, U.K., 316, 1994.

Guo, J.,Y. Miao, Y. Zhang, H. Liu, Z. Li, W. Zhang, J. He, M. Lou, Y. Yan, L. Bian, and P. Zhai: The climatology of planetary boundary layer height in China derived from radiosonde and reanalysis data, Atmos. Chem. Phys., 16(20), 13309-13319, doi:10.5194/acp-16-13309-2016, 2016.

Guo, J., X. Zhang, Y. Wu, H. Che, Laba, and X. Li: Spatio-temporal variation trends of satellite-based aerosol optical depth in China during 1980-2008, Atmos. Environ., 45(37), 6802-6811,doi: 10.1016/j.atmosenv.2011.03.068,2011.

He, Q. and Mao, J.: Observation of urban mixed layer at Beijing using a micro pulse lidar, Acta Meteorol. Sin., 63, 374–384, 2005.

Hu M., S. Liu, Z. J. Wu, J. Zhang, Y. L. Zhao, W. Birgit, and W. Alfred: Effects of high temperature, high relative humidity and rain process on particle size distributions in the summer of Beijing, Environ. Sci., 27(11), 2006.

Hu, X., Ma, Z., Lin, W., Zhang, H., Hu, J., Wang, Y., Xu, X., Fuentes, J. D. and Xue, M.: Impact of the Loess Plateau on the atmospheric boundary layer structure and air quality in the North China Plain?: A case study, Sci. Total Environ., 499, 228–237, doi:10.1016/j.scitotenv.2014.08.053, 2014.

Jacobson, M.: Strong radiative heating due to the mixing state of black carbon in atmospheric aerosols, Nature, 409,695-697, 2001.

Ji, D., Y. Wang, L. Wang, L. Chen, B. Hu, G. Tang, J. Xin, T. Song, T. Wen, Y. Sun, Y. Pan, Z. Liu: Analysis of heavy pollution episodes in selected cities of northern China, Atmos. Environ., 50(2012), 338-348, 2012.

Li M., G. Tang, J. Huang, Z. Liu, J. An, and Y. Wang: Relationship between atmospheric MLH and winter haze pollution in the Jing-Jin-Ji region, Environ. Sci., 2015,(06):1935-1943, 2015.

Li, P., J. Xin, X. Bai, Y. Wang, S. Wang, S. Liu, and X. Feng: Observational studies and a statistical early warning of surface ozone pollution in Tangshan, the largest heavy industry city of North China, Inter. J. Env. Res. Pub. Heal., 10(3), 1048-1061, doi:10.3390/ijerph10031048, 2013.

Li, Z., et al.: Aeosol and monsoon climate interactions over Asia, Rev. Geophys., 54, 886-929, doi:10.1002/2015RG000500, 2016.

Liu Z., Y. Sun, L. Li and Y. S. Wang: Particle mass concentrations and size

带格式的：缩进：左侧： 0 厘米，悬挂缩进： 2 字符，首行缩进： -2 字符

带格式的：正文，左，定义网格后不调整右缩进，不调整西文与中文之间的空格，不调整中文和数字之间的空格

带格式的

distribution during and after the Beijing Olympic Games, Environ. Sci., 32(4), doi:10.13227/j.hjkx.2011.04.015, 2011.
Liu, Z., B. Hu, J. Zhang, Y. Yu, and Y. Wang: Characteristics of aerosol size distributions and chemical compositions during wintertime pollution episodes in Beijing, Atmos. Res., 168, 1-12, doi:10.1016/j.atmosres.2015.08.013, 2016.
Miao, Y., X.-M. Hu, S. Liu, T. Qian, M. Xue, Y. Zheng, and S. Wang: Seasonal variation of local atmospheric circulations and boundary layer structure in the Beijing-Tianjin-Hebei region and implications for air quality, J. Adv. Model. Earth. Sy. , 7(4), 1602-1626, doi:10.1002/2015ms000522, 2015.
Münkel, C., and J. Räsänen: New optical concept for commercial lidar ceilometers scanning the boundary layer, P.SPIE, 5571, 364-374, 2004.
Münkel, C., N. Eresmaa, J. Räsänen, and A. Karppinen: Retrieval of mixing height and dust concentration with lidar ceilometer, Bound.-Lay. Meteorol., 124(1), 117-128, doi:10.1007/s10546-006-9103-3, 2007.
Muñoz, R., and A. Undurraga: Daytime Mixing layer over the Santiago Basin: Description of Two Years of Observations with a Lidar Ceilometer, J. Appl. Meteorol. Clim., 49(8), 1728-1741, doi:10.1175/2010jamc2347.1, 2010.
Peng, J., M. Hu, S. Guo, Z. Du, J. Zheng, D. Shang, M. L. Zamora, L. Zeng, M. Shao, Y. Wu, J. Zheng, Y. Wang, C. R. Glen, D. R. Collins, M. J. Molina, and R. Zhang: Markedly enhanced absorption and direct radiative forcing of black carbon under polluted urban environments, P. Natl. Acad. Sci. Usa., 113(4266-4271), doi:10.1073/pnas.1602310113, 2016.
Puygrenier, V., F. Lohou, B. Campistron, F. Saïd, G. Pigeon, B. Bénech, and D. Serça: Investigation on the fine structure of sea-breeze during ESCOMPTE experiment, Atmos. Res., 74(1–4), 329-353, doi:http://dx.doi.org/10.1016/j.atmosres.2004.06.011, 2005.
Quan, J., Gao, Y., Zhang, Q., Tie, X., Cao, J., Han, S., Meng, J., Chen, P., and Zhao, D.: Evolution of planetary boundary layer under different weather conditions, and its impact on aerosol concentrations, Particuology, 11, 34–40, doi:10.1016/j.partic.2012.04.005, 2013.
Schween, J., A. Hirsikko, U. Löhnert, and S. Crewell: Mixing-layer height retrieval with ceilometer and Doppler lidar: from case studies to long-term assessment, Atmos. Meas. Tech., 7(11), 3685-3704, doi:10.5194/amt-7-3685-2014, 2014.
Seibert, P., F. Beyrich, S.-E. Gryning, S. Joffre, A. Rasmussen, and P. Tercier: Review and intercomparison of operational methods for the determination of the mixing height, Atmos. Environ., 34(7), 1001-1027, doi:http://dx.doi.org/10.1016/S1352-2310(99)00349-0, 2000.
Seidel, D. J., C. O. Ao, and K. Li: Estimating climatological planetary boundary layer heights from radiosonde observations: Comparison of methods and uncertainty analysis, J. Geophys. Res., 115, D16113, doi:10.1029/2009JD013680, 2010.
Seinfeld J. and S.N. Pandis: Atmospheric Chemistry and Physics: From Air Pollution to Climate Change, New York: John Wiley and Sons, 1998.
Sicard, M., Pérez, C., Rocadenbosch, F., Baldasano, J.M., and D. García-Vizcaino: Mixed-Layer Depth Determination in the Barcelona Coastal Area From Regular

带格式的: 缩进: 左侧: 0 厘米, 悬挂缩进: 2 字符, 首行缩进: -2 字符

带格式的: EndNote Bibliography, 两端对齐, 缩进: 左侧: 0 厘米, 悬挂缩进: 2 字符, 首行缩进: -2 字符, 定义网格后自动调整右缩进, 调整中文与西文文字的间距, 调整中文与数字的间距

Lidar Measurements: Methods, Results and Limitations. Boundary-Layer Meteorology 119, 135-157, 2006.

Sokół, P., I. Stachlewska, I. Ungureanu, and S. Stefan: Evaluation of the boundary layer morning transition using the CL-31 ceilometer signals, Acta Geophys., 62(2), doi:10.2478/s11600-013-0158-5, 2014.

Stull, R.: An Introduction to Boundary Layer Meteorology, Kluwer Academic Publishers, Dordrecht, 1988.

Su F., M. Yang, J. Zhong, Z. Zhang: The effects of synoptic type on regional atmospheric contamination in North Chian, Res. Of Environ. Sci., 17(3), doi:10.13198/j.res.2004.03.18.sufq.006, 2004.

Tang, G., J. Zhang, X. Zhu, T. Song, C. Münkel, B. Hu, K. Schäfer, Z. Liu, J. Zhang, L. Wang, J. Xin, P. Suppan, and Y. Wang: Mixing layer height and its implications for air pollution over Beijing, China, Atmos. Chem. Phys., 16(4), 2459-2475, doi:10.5194/acp-16-2459-2016, 2016.

Tang, G., P. Zhao, Y. Wang, W. Gao, M. Cheng, J. Xin, X. Li, Y. Wang: Mortality and air pollution in Beijing: the long-term relationship. Atmos. Environ., 150, 238-243, doi: 10.1016/j.atmosenv.2016.11.045, 2017a.

Tang, G., X. Li, Y. Wang, J. Xin, and X. Ren: Surface ozone trend details and interpretations in Beijing, 2001–2006, Atmos. Chem. Phys., 9, 8813-8823, doi:10.5194/acp-9-8813-2009, 2009.

Tang, G., X. Zhu, B. Hu, J. Xin, L. Wang, C. Münkel, G. Mao, and Y. Wang: Impact of emission controls on air quality in Beijing during APEC 2014: lidar ceilometer observations, Atmos. Chem. Phys., 15(21), 12667-12680, doi:10.5194/acp-15-12667-2015, 2015.

Tang, G., X. Zhu, J. Xin, B. Hu, T. Song, Y. Sun, J. Zhang, L. Wang, M. Cheng, N. Chao, L. Kong, X. Li, Y Wang. Modelling study of boundary-layer ozone over northern China - Part I: Ozone budget in summer. Atmos. Res., 187, 128-137, 2017b.

Tang, G., Y. Wang, X. Li, D. Ji, S. Hsu, and X. Gao: Spatial-temporal variations in surface ozone in Northern China as observed during 2009–2010 and possible implications for future air quality control strategies, Atmos. Chem. Phys., 12, 2757-2776, doi:10.5194/acp-12-2757-2012, 2012.

Tomasi, F., M. M. Miglietta, M. R. Perrone: The Growth of the Planetary Boundary Layer at a Coastal Site: a Case Study, Bound.-Lay. Meteorol., 139:521-541, doi: 10.1007/s10546-011-9592-6, 2011.

Tu J., S. Zhang, X. Cheng, W. Yang, Y. Yang: Temporal and Spatial Variation of Atmospheric Boundary Layer Height(ABLH) over the Yellow East China Sea, J. Ocean U. China, 42(4):7-18, 2012.

Kamp, V. and I. McKendry: Diurnal and Seasonal Trends in Convective Mixed-Layer Heights Estimated from Two Years of Continuous Ceilometer Observations in Vancouver, BC, Bound.-Lay. Meteorol., 137(3), 459-475, doi:10.1007/s10546-010-9535-7, 2010.

Nair, V., K. Moorthy, D. Alappattu, P. Kunhikrishnan, S. George, P. Nair, S. Babu, B. Abish, S. Satheesh, S. Tripathi, K. Niranjan, B. Madhavan, V. Srikant, C. Dutt, K.

带格式的：缩进：左侧： 0 厘米，悬挂缩进：2 字符，首行缩进： -2 字符

Badarinath, and R. Reddy: Wintertime aerosol characteristics over the Indo-Gangetic Plain (IGP): Impacts of local boundary layer processes and long-rang transport, J. Geo. Res.: 2006JD008099, doi:10.1029/2006JD008099, 2007.

Wagner, M., S. Emeis, V. Freudenthaler, B. Heese, W. Junkermann, C. Münkel, K. Schäfer, M. Seefeldner, and S. Vogt: Mixing layer height over Munich, Germany: Variability and comparisons of different methodologies, J. Geophys. Res., 111, D13201, doi:10.1029/2005JD006593, 2006.

Wagner, P., K. Schäfer: Influence of mixing layer height on air pollutant concentrations in an urban street canyon, Urban Climate, http://dx.doi.org/10.1016/j.uclim.2015.11.001, 2015.

Wang, L., N. Zhang, Z. Liu, Y. Sun, D. Ji, and Y. Wang: The Influence of Climate Factors, Meteorological Conditions, and Boundary-Layer Structure on Severe Haze Pollution in the Beijing-Tianjin-Hebei Region during January 2013, Adv. Meteorol., 2014, 1-14, doi:10.1155/2014/685971, 2014.

Wang, Y., L. Yao, L. Wang, Z. Liu, D. Ji, G. Tang, J. Zhang, Y. Sun, B. Hu, and J. Xin: Mechanism for the formation of the January 2013 heavy haze pollution episode over central and eastern China, Sci. China Earth Sci., 57(1), 14-25, doi:10.1007/s11430-013-4773-4, 2013a.

Wang, Y., M. L. Zamora, and R. Zhang: New Directions: Light absorbing aersols and their atmospheric impacts, Atmos. Environ., 81, 713-715, doi: 10.1016/j.atmosenv.2013.09.034, 2013b.

Wei, J., G. Tang, X. Zhu, L. Wang, Z. Liu, M. Cheng, C. Münkel, X. Li, Y. Wang: Thermal internal boundary layer and its effects on air pollutants during summer in a coastal city in North China, Journal of Environmental Sciences, 1001-0742, doi:10.1016/j.jes.2017.11.006, 2017.

Wiegner, M., F. Madonna, I. Binietoglou, R. Forkel, J. Gasteiger, A. Geiβ, G. Pappalardo, K. Schäfer, and W. Thomas: What is the benefit of ceilometers for aerosol remote sensing? An answer from ERALINET, Atmos. Meas. Tech., 7, 1979-1997, doi: 10.5194/amt-7-1979-2014, 2014.

Xu, R., G. Tang, Y. Wang, and X. Tie: Analysis of a long-term measurement of air pollutants (2007-2011) in North China Plain (NCP); Impact of emission reduction during the Beijing Olympic Games, Chemosphere, 159, 647-658, doi:10.1016/j.chemosphere.2016.06.025, 2016.

Yu, H., S. Liu, and R. Dickinson: Radiative effects of aerosols on the evolution of the atmospheric boundary layer, J. Geo. Res.: Atmos., 107, D12(4142), doi:10.1029/2001JD000754, 2002.Zhang Z., X. Cai, Y. Song, L. Kang, X. Huang, Q. Li: Temporal and spatial variation of atmospheric boundary layer height over Hainan Island and its adjacent sea areas, Acta. Sci. Nat. Univ. Pekin., 49:83-90, doi: 10.13209/j.0479-8023.2013.105, 2013.

Zhang, H., Y. Wang, J. Hu, Q. Ying, and X.-M. Hu: Relationships between meteorological parameters and criteria air pollutants in three megacities in China, Environ. Res., 140, 242–254, doi:10.1016/j.envres.2015.04.004, 2015a.

Zhang, J. K., Y. Sun, Z. R. Liu, D. S. Ji, B. Hu, Q. Liu, and Y. S. Wang:

带格式的: 正文，左，缩进：左侧：0 厘米，悬挂缩进：2.5 字符，首行缩进：-2.5 字符，定义网格后不调整右缩进，不调整西文与中文之间的空格，不调整中文和数字之间的空格

带格式的: 英语(英国)

Characterization of submicron aerosols during a month of serious pollution in Beijing, 2013, Atmos. Chem. Phys., 14(6), 2887-2903, doi:10.5194/acp-14-2887-2014, 2014.

Zhang, Q., J. Xin, Y. Yin, L. Wang, and Y. Wang: The Variation and Trends of MODIS C5 & C6 Products' Errors in the Recent Decade over the Background and Urban Areas of North China, Remote Sensing, 8(9), 754, doi:10.3390/rs8090754, 2016b.

Zhang, R., G. Hui, S. Guo, M. L. Zamora, Q. Ying, Y. Lin, W. Wang, M. Hu, and Y. Wang: Formation of Urban Fine Particulate Matter, Chem. Rev., 115, 3803-3855, doi: 10.1021/acs.chemrev.5b00067, 2015b.

Zhang, R.: Getting to the Critical Nucleus of Aerosol Formation, Science, 328(5984), 1366-1367, doi: 10.1126/science.1189732, 2010.

Zhang, W., J. Guo, Y. Miao, H. Liu, Y. Zhang, Z. Li, and P. Zhai: Planetary boundary layer height from CALIOP compared to radiosonde over China, Atmos. Chem. Phys., 16, 9951–9963, doi: 10.5194/acp-16-9951-2016, 2016a.

Zhao, X., P. Zhao, J. Xu, W. Meng, W. Pu, F. Dong, D. He, and Q. Shi: Analysis of a winter regional haze event and its formation mechanism in the North China Plain, Atmos. Chem. Phys., 13 (11), 5685-5696, 2013.

Zhu, X., G. Tang, B. Hu, L. Wang, J. Xin, J. Zhang, Z. Liu, C. Münkel, and Y. Wang: Regional pollution and its formation mechanism over North China Plain: A case study with ceilometer observations and model simulations, J. Geo. Res.: Atmos., 2016JD025730, doi:10.1002/2016JD025730, 2016.

Beyrich, F.: Mixing height estimation from SODAR data – a critical discussion, Atmos. Environ., 31, 3941–3953, 1997.

Bond, T. C., et al.: Bounding the role of black carbon in the climate system: a scientific assessment, J. Geophys. Res., 118, 1-173, doi:10.1002/jgrd.50171, 2013.

Chen, W., Kuze, H., Uchiyama, A., Suzuki, Y., and Takeuchi, N.: One-year observation of urban mixed layer characteristics at Tsukuba, Japan using a micro pulse lidar, Atmos. Environ., 35, 4273–4280, doi:10.1016/S1352-2310(01)00181-9, 2001.

Emeis, S., C. Münkel, S. Vogt, W. J. Müller, and K. Schäfer: Atmospheric boundary-layer structure from simultaneous SODAR, RASS, and ceilometer measurements, Atmos. Environ., 38(2), 273-286, doi:10.1016/j.atmosenv.2003.09.054, 2004.

Emeis, S., K. Schäfer, and C. Münkel: Observation of the structure of the urban boundary layer with different ceilometers and validation by RASS data, Meteorologische Zeitschrift, 18(2), 149-154, doi:10.1127/0941-2948/2009/0365, 2009.

Emeis, S., K. Schäfer, C. Münkel, R. Friedl, and P. Suppan: Evaluation of the Interpretation of Ceilometer Data with RASS and Radiosonde Data, Bound.-Lay. Meteorol., 143(1), 25-35, doi:10.1007/s10546-011-9604-6, 2011.

Eresmaa, N., Karppinen, A., Joffre, S. M., Räsänen, J., and Talvitie, H.: Mixing height

带格式的: 缩进: 左侧: 0 厘米, 悬挂缩进: 2 字符, 首行缩进: -2 字符

determination by ceilometer, Atmos. Chem. Phys., 6, 1485-1493, doi: 10.5194/acp-6-1485-2006, 2006.

Fu, G., W. Xu, R. Yang, J. Li, and C. Zhao: The distribution and trends of fog and haze in the North China Plain over the past 30 years, Atmos. Chem. Phys., 14 (21), 11949-11958, 2014.

Garratt JR, The atmospheric boundary layer. Cambridge University Press, U.K., 316, 1994.

Guo, J.,Y. Miao, Y. Zhang, H. Liu, Z. Li, W. Zhang, J. He, M. Lou, Y. Yan, L. Bian, and P. Zhai: The climatology of planetary boundary layer height in China derived from radiosonde and reanalysis data, Atmos. Chem. Phys., 16(20), 13309-13319, doi:10.5194/acp-16-13309-2016, 2016.

Guo, J.P., X.Y. Zhang, Y.R. Wu, H.Z. Che, Laba, and X. Li: Spatio-temporal variation trends of satellite-based aerosol optical depth in China during 1980-2008, Atmos. Environ., 45(37), 6802-6811,doi: 10.1016/j.atmosenv.2011.03.068,2011.

He, Q. and Mao, J.: Observation of urban mixed layer at Beijing using a micro pulse lidar, Acta Meteorol. Sin., 63, 374–384, 2005.

Hu, X., Ma, Z., Lin, W., Zhang, H., Hu, J., Wang, Y., Xu, X., Fuentes, J. D. and Xue, M.: Impact of the Loess Plateau on the atmospheric boundary layer structure and air quality in the North China Plain?: A case study, Sci. Total Environ., 499, 228–237, doi:10.1016/j.scitotenv.2014.08.053, 2014.

Jacobson, M. Z.: Strong radiative heating due to the mixing state of black carbon in atmospheric aerosols, Nature, 409,695-697, 2001.

Ji, D., Y. Wang, L. Wang, L. Chen, B. Hu, G. Tang, J. Xin, T. Song, T. Wen, Y. Sun, Y. Pan, Z. Liu: Analysis of heavy pollution episodes in selected cities of northern China, Atmos. Environ., 50(2012), 338-348, 2012.

Li M., G. Tang, J. Huang, Z. Liu, J. An, and Y. Wang: Relationship between atmospheric MLH and winter haze pollution in the Jing-Jin-Ji region, Environ. Sci., 2015,(06):1935-1943, 2015.

Li, P., J. Xin, X. Bai, Y. Wang, S. Wang, S. Liu, and X. Feng: Observational studies and a statistical early warning of surface ozone pollution in Tangshan, the largest heavy industry city of North China, Inter. J. Env. Res. Pub. Heal., 10(3), 1048-1061, doi:10.3390/ijerph10031048, 2013.

Li, Z., et al.: Aeosol and monsoon climate interactions over Asia, Rev. Geophys., 54, 886-929, doi:10.1002/2015RG000500, 2016.

Liu, Z., B. Hu, J. Zhang, Y. Yu, and Y. Wang: Characteristics of aerosol size distributions and chemical compositions during wintertime pollution episodes in Beijing, Atmos. Res., 168, 1-12, doi:10.1016/j.atmosres.2015.08.013, 2016.

Miao, Y., X.-M. Hu, S. Liu, T. Qian, M. Xue, Y. Zheng, and S. Wang: Seasonal variation of local atmospheric circulations and boundary layer structure in the Beijing-Tianjin-Hebei region and implications for air quality, J. Adv. Model. Earth. Sy. , 7(4), 1602-1626, doi:10.1002/2015ms000522, 2015.

Münkel, C., and J. Räsänen: New optical concept for commercial lidar ceilometers scanning the boundary layer, P.SPIE, 5571, 364-374, 2004.

Münkel, C., N. Eresmaa, J. Räsänen, and A. Karppinen: Retrieval of mixing height

带格式的：缩进：左侧： 0 厘米，悬挂缩进：2 字符，首行缩进： -2 字符

and dust concentration with lidar ceilometer, Bound.-Lay. Meteorol., 124(1), 117-128, doi:10.1007/s10546-006-9103-3, 200.

Muñoz, R. C., and A. A. Undurraga: Daytime Mixing layer over the Santiago Basin: Description of Two Years of Observations with a Lidar Ceilometer, J. Appl. Meteorol. Clim., 49(8), 1728-1741, doi:10.1175/2010jamc2347.1, 2010.

Peng, J., M. Hu, S. Guo, Z. Du, J. Zheng, D. Shang, M. L. Zamora, L. Zeng, M. Shao, Y. Wu, J. Zheng, Y. Wang, C. R. Glen, D. R. Collins, M. J. Molina, and R. Zhang: Markedly enhanced absorption and direct radiative forcing of black carbon under polluted urban environments, P. Natl. Acad. Sci. Usa., 113(4266-4271), doi:10.1073/pnas.1602310113, 2016.

Puygrenier, V., F. Lohou, B. Campistron, F. Saïd, G. Pigeon, B. Bénech, and D. Serça: Investigation on the fine structure of sea-breeze during ESCOMPTE experiment, Atmos. Res., 74(1-4), 329-353, doi:http://dx.doi.org/10.1016/j.atmosres.2004.06.011, 2005.

Quan, J., Gao, Y., Zhang, Q., Tie, X., Cao, J., Han, S., Meng, J., Chen, P., and Zhao, D.: Evolution of planetary boundary layer under different weather conditions, and its impact on aerosol concentrations, Particuology, 11, 34-40, doi:10.1016/j.partic.2012.04.005, 2013.

Schween, J. H., A. Hirsikko, U. Löhnert, and S. Crewell: Mixing-layer height retrieval with ceilometer and Doppler lidar: from case studies to long-term assessment, Atmos. Meas. Tech., 7(11), 3685-3704, doi:10.5194/amt-7-3685-2014, 2014.

Seibert, P., F. Beyrich, S.-E. Gryning, S. Joffre, A. Rasmussen, and P. Tercier: Review and intercomparison of operational methods for the determination of the mixing height, Atmos. Environ., 34(7), 1001-1027, doi:http://dx.doi.org/10.1016/S1352-2310(99)00349-0, 2000.

Seidel, D. J., C. O. Ao, and K. Li: Estimating climatological planetary boundary layer heights from radiosonde observations: Comparison of methods and uncertainty analysis, J. Geophys. Res., 115, D16113, doi:10.1029/2009JD013680, 2010.

Sicard, M., Pérez, C., Rocadenbosch, F., Baldasano, J.M., and D. García-Vizcaino: Mixed-Layer Depth Determination in the Barcelona Coastal Area From Regular Lidar Measurements: Methods, Results and Limitations. Boundary-Layer Meteorology 119, 135-157, 2006.

Sokół, P., I. Stachlewska, I. Ungureanu, and S. Stefan: Evaluation of the boundary layer morning transition using the CL-31 ceilometer signals, Acta Geophys., 62(2), doi:10.2478/s11600-013-0158-5, 2014.

Stull, R.B.: An Introduction to Boundary Layer Meteorology, Kluwer Academic Publishers, Dordrecht, 1988.

Su F.Q., M.Z. Yang, J.H. Zhong, Z.G. Zhang: The effects of synoptic type on regional atmospheric contamination in North Chian, Res. Of Environ. Sci., 17(3), doi:10.13198/j.res.2004.03.18.sufq.006, 2004.

Tang, G., J. Zhang, X. Zhu, T. Song, C. Münkel, B. Hu, K. Schäfer, Z. Liu, J. Zhang, L. Wang, J. Xin, P. Suppan, and Y. Wang: Mixing layer height and its implications for air pollution over Beijing, China, Atmos. Chem. Phys., 16(4), 2459-2475, doi:10.5194/acp-16-2459-2016, 2016.

带格式的: EndNote Bibliography, 两端对齐, 缩进: 左侧: 0 厘米, 悬挂缩进: 2 字符, 首行缩进: -2 字符, 定义网格后自动调整右缩进, 调整中文与西文文字的间距, 调整中文与数字的间距

带格式的: 缩进: 左侧: 0 厘米, 悬挂缩进: 2 字符, 首行缩进: -2 字符

Tang, G., P. Zhao, Y. Wang, W. Gao, M. Cheng, J. Xin, X. Li, Y. Wang: Mortality and air pollution in Beijing: the long-term relationship. Atmos. Environ., 150, 238-243, doi: 10.1016/j.atmosenv.2016.11.045, 2017a.
Tang, G., X. Li, Y. Wang, J. Xin, and X. Ren: Surface ozone trend details and interpretations in Beijing, 2001-2006, Atmos. Chem. Phys., 9, 8813-8823, doi:10.5194/acp-9-8813-2009, 2009.
Tang, G., X. Zhu, B. Hu, J. Xin, L. Wang, C. Münkel, G. Mao, and Y. Wang: Impact of emission controls on air quality in Beijing during APEC 2014: lidar ceilometer observations, Atmos. Chem. Phys., 15(21), 12667-12680, doi:10.5194/acp-15-12667-2015, 2015.
Tang, G., X. Zhu, J. Xin, B. Hu, T. Song, Y. Sun, J. Zhang, L. Wang, M. Cheng, N. Chao, L. Kong, X. Li, Y Wang. Modelling study of boundary-layer ozone over northern China - Part I: Ozone budget in summer. Atmos. Res., 187, 128-137, 2017b.
Tang, G., Y. Wang, X. Li, D. Ji, S. Hsu, and X. Gao: Spatial-temporal variations in surface ozone in Northern China as observed during 2009-2010 and possible implications for future air quality control strategies, Atmos. Chem. Phys., 12, 2757-2776, doi:10.5194/acp-12-2757-2012, 2012.
Tomasi, F. D., M. M. Miglietta, M. R. Perrone: The Growth of the Planetary Boundary Layer at a Coastal Site: a Case Study, Bound.-Lay. Meteorol., 139:521-541, doi: 10.1007/s10546-011-9592-6, 2011.
Tu J., S. Zhang, X. Cheng, W. Yang, Y. Yang: Temporal and Spatial Variation of Atmospheric Boundary Layer Height(ABLH) over the Yellow East China Sea, J. Ocean U. China, 42(4):7-18, 2012.
van der Kamp, D., and I. McKendry: Diurnal and Seasonal Trends in Convective Mixed-Layer Heights Estimated from Two Years of Continuous Ceilometer Observations in Vancouver, BC, Bound.-Lay. Meteorol., 137(3), 459-475, doi:10.1007/s10546-010-9535-7, 2010.
Vijayakumar S. Nair, K. K. Moorthy, D. P. Alappattu, P. K. Kunhikrishnan, S. George, P. R. Nair, S. S. Babu, B. Abish, S. K. Satheesh, S. N. Tripathi, K. Niranjan, B. L. Madhavan, V. Srikant, C. B. S. Dutt, K. V. S. Badarinath, and R. R. Reddy: Wintertime aerosol characteristics over the Indo-Gangetic Plain (IGP): Impacts of local boundary layer processes and long-rang transport, J. Geo. Res.: 2006JD008099, doi:10.1029/2006JD008099, 2007.
Wagner, P., K. Schäfer: Influence of mixing layer height on air pollutant concentrations in an urban street canyon, Urban Climate, http://dx.doi.org/10.1016/j.uclim.2015.11.001, 2015.
Wang, L., N. Zhang, Z. Liu, Y. Sun, D. Ji, and Y. Wang: The Influence of Climate Factors, Meteorological Conditions, and Boundary-Layer Structure on Severe Haze Pollution in the Beijing-Tianjin-Hebei Region during January 2013, Adv. Meteorol., 2014, 1-14, doi:10.1155/2014/685971, 2014.
Wang, Y., L. Yao, L. Wang, Z. Liu, D. Ji, G. Tang, J. Zhang, Y. Sun, B. Hu, and J. Xin: Mechanism for the formation of the January 2013 heavy haze pollution episode over central and eastern China, Sci. China Earth Sci., 57(1), 14-25,

doi:10.1007/s11430-013-4773-4, 2013.

Wang, Y., M. L. Zamora, and R. Zhang: New Directions: Light absorbing aerosols and their atmospheric impacts, Atmos. Environ., 81, 713-715, doi: 10.1016/j.atmosenv.2013.09.034, 2013.

Wiegner, M., F. Madonna, I. Binietoglou, R. Forkel, J. Gasteiger, A. Geiβ, G. Pappalardo, K. Schäfer, and W. Thomas: What is the benefit of ceilometers for aerosol remote sensing? An answer from ERALINET, Atmos. Meas. Tech., 7, 1979-1997, doi: 10.5194/amt-7-1979-2014, 2014.

Xu, R., G. Tang, Y. Wang, and X. Tie: Analysis of a long-term measurement of air pollutants (2007-2011) in North China Plain (NCP); Impact of emission reduction during the Beijing Olympic Games, Chemosphere, 159, 647-658, doi:10.1016/j.chemosphere.2016.06.025, 2016.

Yu, H., S. Liu, and R. Dickinson: Radiative effects of aerosols on the evolution of the atmospheric boundary layer, J. Geo. Res.: Atmos., 107, D12(4142), doi:10.1029/2001JD000754, 2002.Zhang Z., X. Cai, Y. Song, L. Kang, X. Huang, Q. Li: Temporal and spatial variation of atmospheric boundary layer height over Hainan Island and its adjacent sea areas, Acta. Sci. Nat. Univ. Pekin., 49:83-90, doi: 10.13209/j.0479-8023.2013.105, 2013.

Zhang, H., Y. Wang, J. Hu, Q. Ying, and X. M. Hu: Relationships between meteorological parameters and criteria air pollutants in three megacities in China, Environ. Res., 140, 242–254, doi:10.1016/j.envres.2015.04.004, 2015.

Zhang, J. K., Y. Sun, Z. R. Liu, D. S. Ji, B. Hu, Q. Liu, and Y. S. Wang: Characterization of submicron aerosols during a month of serious pollution in Beijing, 2013, Atmos. Chem. Phys., 14(6), 2887-2903, doi:10.5194/acp-14-2887-2014, 2014.

Zhang, R., G. Hui, S. Guo, M. L. Zamora, Q. Ying, Y. Lin, W. Wang, M. Hu, and Y. Wang: Formation of Urban Fine Particulate Matter, Chem. Rev., 115, 3803-3855, doi: 10.1021/acs.chemrev.5b00067, 2015.

Zhang, R.: Getting to the Critical Nucleus of Aerosol Formation, Science, 328(5984), 1366-1367, doi: 10.1126/science.1189732, 2010.

Zhang, W., J. Guo, Y. Miao, H. Liu, Y. Zhang, Z. Li, and P. Zhai: Planetary boundary layer height from CALIOP compared to radiosonde over China, Atmos. Chem. Phys., 16, 9951–9963, doi: 10.5194/acp-16-9951-2016, 2016.

Zhao, X., P. Zhao, J. Xu, W. Meng, W. Pu, F. Dong, D. He, and Q. Shi: Analysis of a winter regional haze event and its formation mechanism in the North China Plain, Atmos. Chem. Phys., 13 (11), 5685-5696, 2013.

Zhu, X., G. Tang, B. Hu, L. Wang, J. Xin, J. Zhang, Z. Liu, C. Münkel, and Y. Wang: Regional pollution and its formation mechanism over North China Plain: A case study with ceilometer observations and model simulations, J. Geo. Res.: Atmos., 2016JD025730, doi:10.1002/2016JD025730, 2016.

Liu Z. R., Y. Sun, L. Li and Y. S. Wang: Particle mass concentrations and size distribution during and after the Beijing Olympic Games, Environ. Sci., 32(4), doi:10.13227/j.hjkx.2011.04.015, 2011.

Hu M., S. Liu, Z. J. Wu, J. Zhang, Y. L. Zhao, W. Birgit, and W. Alfred: Effects of

带格式的: 正文, 左, 缩进: 左侧: 0 厘米, 悬挂缩进: 2.5 字符, 首行缩进: -2.5 字符, 定义网格后不调整右缩进, 不调整西文与中文之间的空格, 不调整中文和数字之间的空格

带格式的: 英语(英国)

带格式的: 缩进: 左侧: 0 厘米, 悬挂缩进: 2 字符, 首行缩进: -2 字符

带格式的: 正文, 左, 定义网格后不调整右缩进, 不调整西文与中文之间的空格, 不调整中文和数字之间的空格

high temperature, high relative humidity and rain process on particle size distributions in the summer of Beijing, Environ. Sci., 27(11), 2006.

带格式的

带格式的: 缩进: 左侧: 0 厘米, 悬挂缩进: 2 字符, 首行缩进: -2 字符